G418 (1 mg/mL, Invitrogen). JAK3 was immunoprecipitated from neomycin-resistant mass cultures of 32D-mCAT cells with goat polyclonal antibodies specific for this protein (sc-1078; Santa Cruz Biotechnology, Santa Cruz, CA). Half of the resulting precipitates were subjected to immunoblot analysis with a mouse monoclonal antibody to phosphotyrosine (4G-10; Upstate Biotechnology, Charlottesville, VA) or rabbit polyclonal antibodies to JAK3 (sc-513, Santa Cruz Biotechnology). Antibodies used for the immunoprecipitation of STAT1 were obtained from Upstate Biotechnology, those specific for STAT3 were from Cell Signaling Technology (Danvers, MA), and those specific for STAT5 or STAT6 were from Santa Cruz Biotechnology. Immune complexes on immunoblots were visualized with SuperSignal West Pico Chemiluminescent substrate (Pierce, Rockford, IL).

The remaining half of the immunoprecipitates were then washed with kinase buffer [10 mM HEPES–NaOH (pH 7.4), 50 mM NaCl, 5 mM $MgCl_2$, 5 mM $MnCl_2$, 0.1 mM Na_3VO_4] and then incubated for 30 min at room temperature in 30 μL of the kinase buffer containing 0.37 MBq of [γ-^{32}P]ATP (GE Healthcare Bio-Sciences, Uppsala, Sweden) and 1 μg of a synthetic peptide (LLPLDKDYYVVREPGQS) corresponding to amino acids 973–989 of human JAK3 (Operon Biotechnologies, Huntsville, AL).

3. Results

3.1. Screening for transforming genes in 32D-mCAT cells

To isolate transforming genes from a retroviral expression library, we used mouse 32Dcl3 cells, which proliferate in the presence of IL-3 but undergo terminal differentiation to granulocytes in response to G-CSF [6]. Introduction of v-Ha-Ras or v-Abl oncogenes into these cells induces continuous growth even in the presence of G-CSF [12,13], indicating that active oncogenes are able to override the differentiation program of 32Dcl3 cells. We thus reasoned that retroviral transduction of transforming genes present in AML blasts into 32Dcl3 cells might also elicit proliferation in the presence of G-CSF. Given that the efficiency of infection of 32Dcl3 cells with ecotropic retroviruses was low (<2%), we generated 32D-mCAT cells, which overexpress an ecotropic retrovirus receptor and exhibit an infection efficiency of 10–30% (data not shown). We then examined the feasibility of a novel screening system for transforming genes that consists of (1) infection of 32D-mCAT cells with recombinant retroviral cDNA libraries constructed from AML specimens, (2) selection of proliferating 32D-mCAT cells in the presence of G-CSF, and (3) isolation of transforming cDNAs by PCR with a primer targeted to a sequence flanking the cDNA in each retrovirus.

3.2. Screening with a retroviral cDNA expression library from an AML patient

To screen for transforming genes in AML, we prepared a CD133$^+$ hematopoietic stem cell-like fraction from an 84-year old Japanese man with AML (M2 subtype according to the FAB classification). The patient had a clinical history of myelodysplastic syndrome prior to the onset of AML, and his malignant blasts had a karyotype of monosomy 7. Purification of a CD133$^+$ immature cell faction likely enriched for

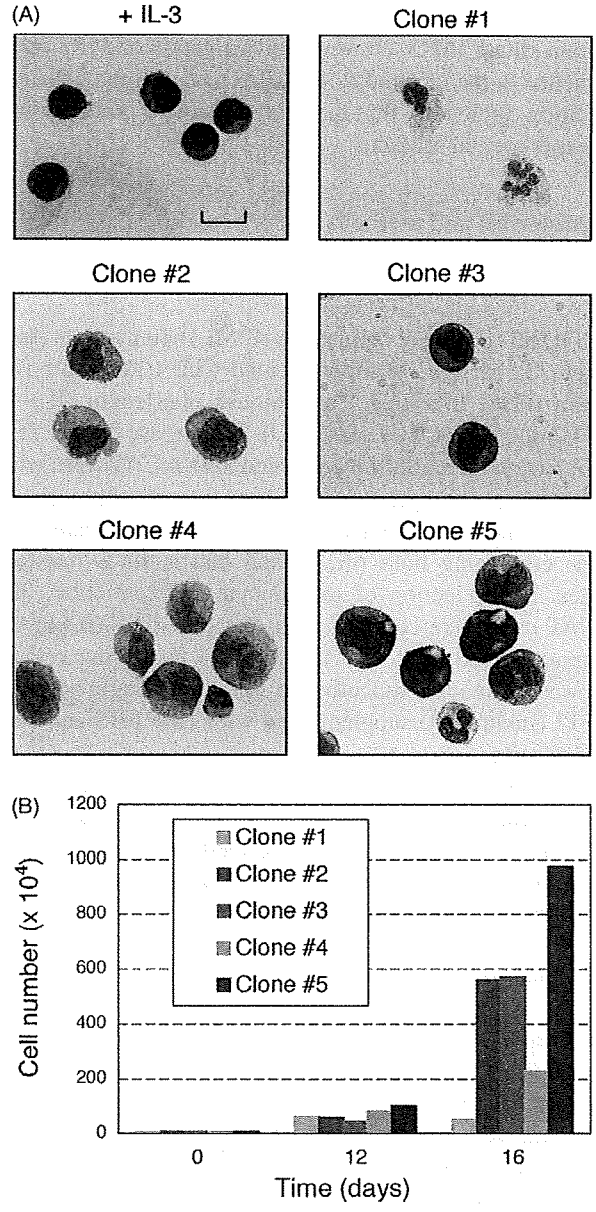

Fig. 1. Isolation of 32D-mCAT clones that proliferate in the presence of G-CSF. (A) 32D-mCAT cells cultured with IL-3 (+IL-3) as well as 32D-mCAT clones infected with the retroviral expression library (clones #1, #2, #3, #4, and #5) and cultured for 16 days with G-CSF were stained with Wright-Giemsa solutions and photographed. Scale bar, 100 μm. (B) Proliferation of 32D-mCAT cells of clones #1 to #5 was determined by counting the cell number after culture with G-CSF for 12 or 16 days. The experiments were repeated twice, and both data were basically identical.

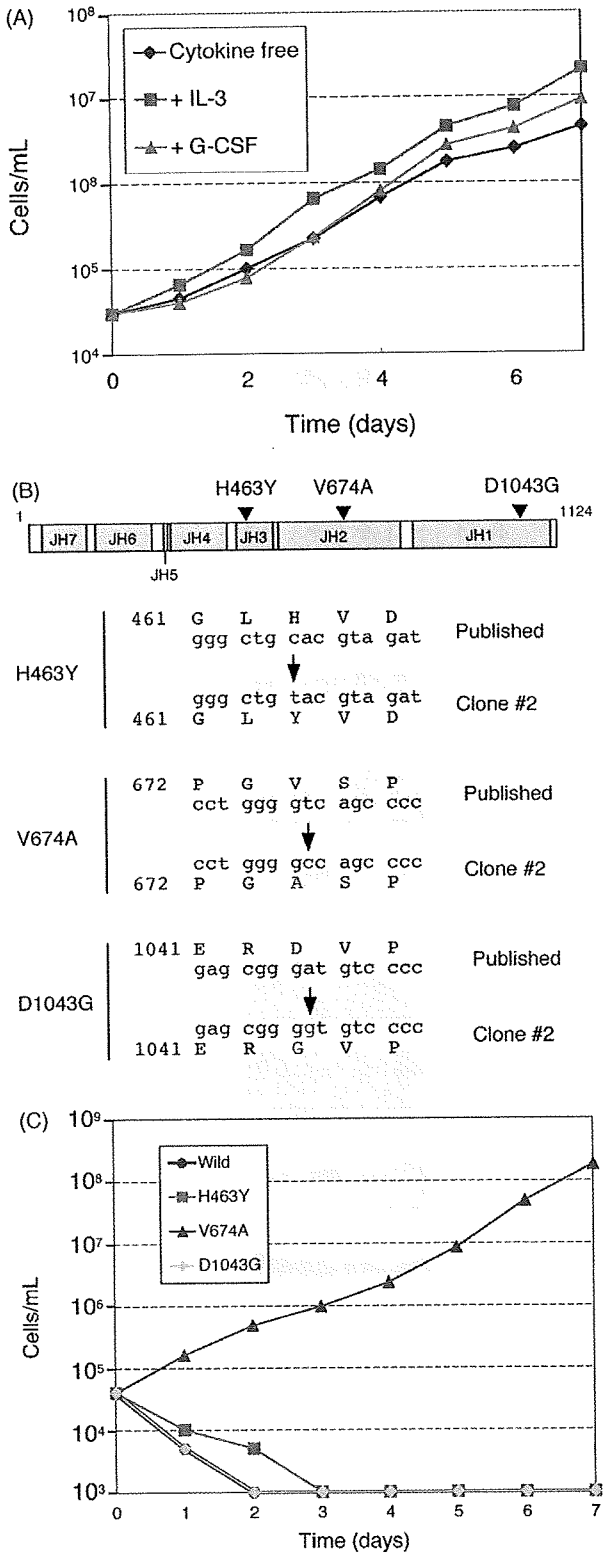

Fig. 2. Expression of JAK3(V674A) abrogates cytokine dependency of 32D-mCAT cell growth. (A) 32D-mCAT cells were infected with recombinant retroviruses containing the *JAK3* cDNA isolated from 32D-mCAT clone #2. The cells were then cultured in the absence or presence of IL-3 or G-CSF, and cell number was counted at the indicated times thereafter. The experiments were repeated twice, and both data were basically identical. (B) Schematic structure of human JAK3 showing the JH domains and the positions of amino acid substitutions encoded by the PCR product obtained from 32D-mCAT clone #2. The corresponding nucleotide changes in the *JAK3* cDNA sequence are shown below. (C) Growth curves for 32D-mCAT cells infected with retroviruses encoding wild-type human JAK3 or the mutants JAK3(H463Y), JAK3(V674A), or JAK3(D1043G) and cultured without cytokine. The experiments were repeated twice, and both data were basically identical.

leukemic clones and helped to eliminate mRNA of normal bone marrow cells [10].

We selectively amplified full-length cDNAs from total RNA of the $CD133^+$ blasts of the patient and ligated them into the retroviral vector pMX. We obtained a total of 8.7×10^6 colony-forming units of independent plasmid clones. To evaluate the quality of the library, we randomly selected 40 clones and examined the incorporated cDNAs. Thirty-four (85%) of the 40 clones contained inserts with an average size of 1.63 kbp, suggesting that the library was of sufficient complexity for the present study.

A recombinant retroviral library was generated from the plasmids and used to infect 32D-mCAT cells. A total of 2.75×10^6 independent retroviral clones was assayed with a total of 8×10^6 32D-mCAT cells. The cells were subsequently cultured for 16 days in the presence of G-CSF. Whereas proliferating 32D-mCAT cells manifested a high nucleus-to-cytoplasm ratio and basophilic cytoplasm (Fig. 1A, +IL-3), incubation with G-CSF for 16 days induced granulocytic differentiation in most of the cells (Fig. 1A, clone #1). Among the 32D-mCAT cells infected with retroviruses, however, we detected four cell clones (clones #2 to #5) that grew rapidly in the presence of G-CSF (Fig. 1A, data not shown). The cells in each clone were expanded and examined for their growth properties in the presence of G-CSF. The proliferation rate (Fig. 1B) as well as differentiation ability (Fig. 1A, data not shown) varied markedly among the clones. Genomic DNA was isolated from each clone and subjected to PCR in order to amplify the retroviral inserts. Nucleotide sequencing of the inserts revealed that those isolated from clones #2 and #3 were derived from human *JAK3* (GenBank accession number, NM_000215), whereas that from clone #5 was derived from *CSF3R* (accession number, NM_000760), which encodes the G-CSF receptor. PCR failed to detect a cDNA insert in cells of clone #4.

3.3. *Identification of constitutively active JAK3(V674A)*

JAK3 is a cytoplasmic tyrosine kinase that plays an important role in T cell development and function [14,15]. Given that constitutively active forms of JAK3 have not been detected previously, we focused on the *JAK3* cDNAs identified by retroviral expression screening. To confirm the transforming activity of the cDNAs, we ligated them into the pMX-ires-neo plasmid for generation of recombinant retroviruses. The retroviruses were used to infect 32D-mCAT cells, which were then subjected to selection with G418. The cells expressing the *JAK3* cDNA derived from clone #2 grew exponentially in the presence of G-CSF or IL-3 (Fig. 2A).

These cells also grew in the absence of cytokine, showing that the JAK3 derived from clone #2 abrogates cytokine dependency of 32Dcl3 cells. Similar results were obtained with the *JAK3* cDNA isolated from clone #3, and both of the *JAK3* cDNAs (from clones #2 and #3) were identical on both ends (5′- and 3′-termini) (data not shown). We thus chose the *JAK3* cDNA from clone #2 for further analysis.

Complete sequencing of the *JAK3* cDNA from clone #2 revealed that it spans nucleotide positions 20–3460 of the published human *JAK3* cDNA (NM_000215). However, four nucleotides within the isolated cDNA do not match those in the published sequence, and three of these unmatched nucleotides affect the corresponding amino acid sequence of JAK3. A nucleotide change at position 1446 (C to T) results in the replacement of a histidine residue at codon 463 with tyrosine; a nucleotide change at position 2080 (T to C) results in the replacement of valine at codon 674 with alanine; and a nucleotide change at position 3187 (A to G) results in the replacement of aspartic acid at codon 1043 with glycine (Fig. 2B).

To examine the role of these amino acid changes in the transforming activity of the *JAK3* cDNA derived from clone #2, we introduced each mutation individually into the wild-type human *JAK3* cDNA. Each mutant cDNA was ligated into pMX-ires-neo for the production of recombinant retroviruses, which were then used to infect 32D-mCAT cells. Culture of the infected cells in the absence of cytokine revealed that those expressing JAK3(V674A), but not those expressing JAK3(H463Y) or JAK3(D1043G), grew exponentially (Fig. 2C), demonstrating that the amino acid change from valine to alanine at position 674 is responsible for the transforming activity of *JAK3* cDNA from clone #2.

Given that amino acid position 674 is within the JH2 region of JAK3, which negatively regulates the kinase activity of the enzyme [16], the V674A mutation might be expected to affect kinase activity and thereby to confer cytokine independence on 32D-mCAT cell growth. To examine this possibility, we immunoprecipitated JAK3 from 32D-mCAT cells expressing the wild-type or V674A form of the enzyme and subjected the precipitates to immunoblot analysis with an antibody to phosphotyrosine. JAK3(V674A) was constitutively phosphorylated irrespective of cell stimulation with IL-3, and the extent of its phosphorylation was markedly greater than that of wild-type JAK3 (Fig. 3A). Immunoblot analysis of the same samples with antibodies to JAK3 confirmed that the differences in the levels of JAK3 tyrosine phosphorylation were not due to differences in the levels of JAK3 expression. To confirm directly that the kinase activity of JAK3(V674A) is increased, we subjected immunoprecipitates of wild-type JAK3 or JAK3(V674A) to an in vitro kinase assay with a synthetic peptide substrate corresponding to the autophosphorylation site within the kinase domain of JAK3. The kinase activity of JAK3(V674A) was indeed found to be markedly greater than that of wild-type JAK3 and was not influenced by cell stimulation with IL-3 (Fig. 3B).

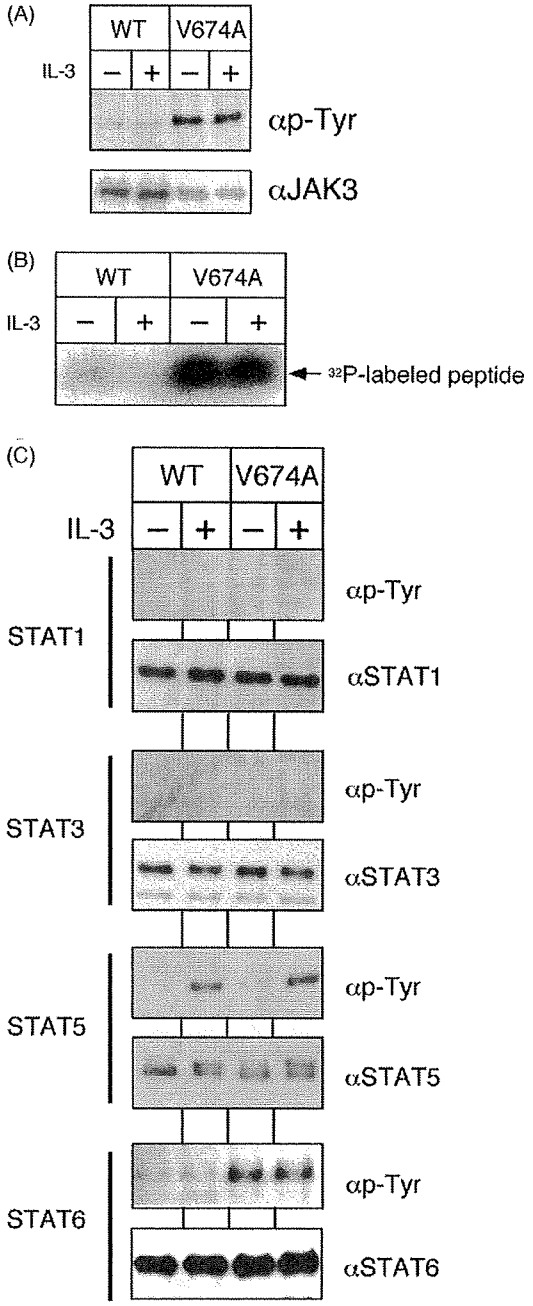

Fig. 3. Constitutive activation of JAK3(V674A). (A) 32D-mCAT cells expressing wild-type JAK3 (WT) or JAK3(V674A) were cultured in the absence of cytokine or FBS for 1 h and then incubated with (+) or without (–) IL-3 for 10 min. Cell lysates were subjected to immunoprecipitation with antibodies to JAK3. Half of the immunoprecipitates were subjected to immunoblot analysis with antibodies to phosphotyrosine (αp-Tyr) or to JAK3 (αJAK3). The experiments were repeated three times, and the data were basically identical. (B) The other half of the precipitates in (A) were subjected to an in vitro kinase assay with a synthetic peptide corresponding to the autophosphorylation site in the kinase domain of JAK3. (C) Cells treated as in (A) were subjected to immunoprecipitation with antibodies to STAT1, STAT3, STAT5, or STAT6, and the resulting precipitates were subjected to immunoblot analysis with antibodies to phosphotyrosine or to the corresponding STAT protein. The experiments were repeated three times, and the data were basically identical.

Signal transducer and activator of transcription (STAT) proteins are important signal transducers for JAK family members [17], and it is known that JAK3 can activate STAT5 and STAT6 in the context of IL-2- and IL-4-signaling systems, respectively. We thus examined the phosphorylation levels of various STATs in 32D-mCAT cells expressing wild-type JAK3 or JAK3(V674A). STAT1, STAT3, STAT5, and STAT6 were immunoprecipitated from such cells and subjected to immunoblot analysis with the antibody to phosphotyrosine. Only STAT6 manifested a higher level of phosphorylation in 32D-mCAT cells expressing JAK3(V674A) than in those expressing the wild-type kinase (Fig. 3C). In addition, STAT6 phosphorylation in the cells expressing JAK3(V674A) was not affected by IL-3, consistent with the lack of effect of this cytokine on the tyrosine phosphorylation of JAK3(V674A). Although STAT5 underwent tyrosine phosphorylation in response to IL-3 stimulation, the magnitude of this effect did not differ between cells expressing wild-type or V674A forms of JAK3 (Fig. 3C).

Finally, to examine whether the nucleotide substitution responsible for the V674A mutation of JAK3 was detectable in the RNA isolated from the AML patient and used for library construction, we amplified a region of *JAK3* cDNA surrounding codon 674 from the unamplified cDNA of the patient and determined its nucleotide sequence. Extensive sequencing failed to detect this nucleotide change, indicating that the activating mutation was artificially generated in the initial PCR step of library construction.

4. Discussion

We have constructed a retroviral cDNA expression library from a patient with AML. The complexity of the library was sufficient to represent most of the transcriptome of the $CD133^+$ cells from which it was prepared. With the use of this retroviral library, we searched for cDNAs whose expression conferred on 32Dcl3 cells the ability to continue proliferating in the presence of G-CSF. Such cDNAs would be expected either (1) to inhibit the differentiation-inducing activity of G-CSF while supporting its mitogenic activity or (2) to possess marked transforming activity. Our screening resulted in the isolation of a cDNA for a constitutively active form of JAK3, which likely conforms to this second possibility.

An activating mutation of *JAK2* was recently identified in blood cells of individuals with myeloproliferative disorders (MPDs) with the exception of chronic myeloid leukemia [18–21]. This JAK2 mutant, JAK2(V617F), possesses an increased kinase activity that is essential for the erythropoietin-independent growth of MPD cell colonies. These observations indicate that some MPD cases are caused by a constitutively active form of JAK2, and that reclassification of MPDs on the basis of transforming events may be required. Amino acid position 617 is localized within the JH2 (pseudokinase) domain of JAK2, which is thought to function as a negative regulatory region for kinase activity [22]. Disruption of JH2 function through point mutations (in addition to that associated with MPDs) has thus been shown to activate JAK2 [23]. The amino acid (valine-674) whose mutation is responsible for the constitutively active form of JAK3 identified in the present study is also located in the JH2 domain of this kinase, emphasizing the importance of this domain in the negative regulation of JAK3. As far as we are aware, oncogenic forms of JAK3 have not previously been described, and mutation of amino acid residues corresponding to valine-674 of JAK3 have not been described for the other JAK family members.

Our inability to detect the corresponding mutation at nucleotide position 2080 in the original *JAK3* cDNA prepared from the AML patient indicates that it was introduced into the retroviral library by the initial PCR step of library construction. This mutation thus does not appear to be related to the molecular pathogenesis of AML in the patient. Similarly, we failed to detect the other two mutations (C1446T and A3187G of *JAK3*) in the original RNA of the patient (data not shown). This observation suggests that care is required to minimize the introduction of artificial mutations in the PCR step for this type of screening and that any mutations identified by such screening should be confirmed by analysis of the original sample. Nevertheless, our identification of an active form of JAK3 demonstrates the potential efficacy of the retroviral library – 32Dcl3 cell screening system for the detection of hematopoietic oncogenes as well as provides insight into the regulation of JAK3 activity.

Acknowledgments

We are thankful to Drs. James N. Ihle and Evan Parganas for their suggestions on the experiments and for their critical reading of this manuscript. This work was supported in part by grants for Research on Human Genome and Tissue Engineering and for Third-Term Comprehensive Control Research for Cancer from the Ministry of Health, Labor, and Welfare of Japan, as well as by a grant for Scientific Research on Priority Areas "Applied Genomics" from the Ministry of Education, Culture, Sports, Science and Technology of Japan.

Contributions. Retrovirus library construction and screening was undertaken by Y.L.C., T.W., S.-I.F., M.S., H.W., and H.H. Construction of mutant JAK3 cDNAs was undertaken by K.K. and M.E., and protein analysis was undertaken by R.K., S.T. and Y.Y. The project was designed by H.M.

References

[1] Kalantry S, Delva L, Gaboli M, Gandini D, Giorgio M, Hawe N, et al. Gene rearrangements in the molecular pathogenesis of acute promyelocytic leukemia. J Cell Physiol 1997;173:288–96.
[2] Moore MA. Converging pathways in leukemogenesis and stem cell self-renewal. Exp Hematol 2005;33:719–37.
[3] Mrozek K, Heerema NA, Bloomfield CD. Cytogenetics in acute leukemia. Blood Rev 2004;18:115–36.

[4] Frohling S, Scholl C, Gilliland DG, Levine RL. Genetics of myeloid malignancies: pathogenetic and clinical implications. J Clin Oncol 2005;23:6285–95.
[5] Aaronson SA. Growth factors and cancer. Science 1991;254: 1146–53.
[6] Greenberger JS, Sakakeeny MA, Humphries RK, Eaves CJ, Eckner RJ. Demonstration of permanent factor-dependent multipotential (erythroid/neutrophil/basophil) hematopoietic progenitor cell lines. Proc Natl Acad Sci USA 1983;80:2931–5.
[7] Choi YL, Moriuchi R, Osawa M, Iwama A, Makishima H, Wada T, et al. Retroviral expression screening of oncogenes in natural killer cell leukemia. Leuk Res 2005;29:943–9.
[8] Albritton LM, Tseng L, Scadden D, Cunningham JM. A putative murine ecotropic retrovirus receptor gene encodes a multiple membrane-spanning protein and confers susceptibility to virus infection. Cell 1989;57:659–66.
[9] Pear WS, Nolan GP, Scott ML, Baltimore D. Production of high-titer helper-free retroviruses by transient transfection. Proc Natl Acad Sci USA 1993;90:8392–6.
[10] Ohmine K, Ota J, Ueda M, Ueno S-I, Yoshida K, Yamashita Y, et al. Characterization of stage progression in chronic myeloid leukemia by DNA microarray with purified hematopoietic stem cells. Oncogene 2001;20:8249–57.
[11] Onishi M, Kinoshita S, Morikawa Y, Shibuya A, Phillips J, Lanier LL, et al. Applications of retrovirus-mediated expression cloning. Exp Hematol 1996;24:324–9.
[12] Mavilio F, Kreider BL, Valtieri M, Naso G, Shirsat N, Venturelli D, et al. Alteration of growth and differentiation factors response by Kirsten and Harvey sarcoma viruses in the IL-3-dependent murine hematopoietic cell line 32D C13(G). Oncogene 1989;4:301–8.
[13] Rovera G, Valtieri M, Mavilio F, Reddy EP. Effect of Abelson murine leukemia virus on granulocytic differentiation and interleukin-3 dependence of a murine progenitor cell line. Oncogene 1987;1:29–35.
[14] Witthuhn BA, Silvennoinen O, Miura O, Lai KS, Cwik C, Liu ET, et al. Involvement of the Jak-3 Janus kinase in signalling by interleukins 2 and 4 in lymphoid and myeloid cells. Nature 1994;370:153–7.
[15] Macchi P, Villa A, Giliani S, Sacco MG, Frattini A, Porta F, et al. Mutations of Jak-3 gene in patients with autosomal severe combined immune deficiency (SCID). Nature 1995;377:65–8.
[16] Saharinen P, Silvennoinen O. The pseudokinase domain is required for suppression of basal activity of Jak2 and Jak3 tyrosine kinases and for cytokine-inducible activation of signal transduction. J Biol Chem 2002;277:47954–63.
[17] Ihle JN, Nosaka T, Thierfelder W, Quelle FW, Shimoda K. Jaks and Stats in cytokine signaling. Stem Cells 1997;15(Suppl 1):105–11 [Discussion 12].
[18] Levine RL, Wadleigh M, Cools J, Ebert BL, Wernig G, Huntly BJ, et al. Activating mutation in the tyrosine kinase JAK2 in polycythemia vera, essential thrombocythemia, and myeloid metaplasia with myelofibrosis. Cancer Cell 2005;7:387–97.
[19] Baxter EJ, Scott LM, Campbell PJ, East C, Fourouclas N, Swanton S, et al. Acquired mutation of the tyrosine kinase JAK2 in human myeloproliferative disorders. Lancet 2005;365:1054–61.
[20] James C, Ugo V, Le Couedic JP, Staerk J, Delhommeau F, Lacout C, et al. A unique clonal JAK2 mutation leading to constitutive signalling causes polycythaemia vera. Nature 2005;434: 1144–8.
[21] Kralovics R, Passamonti F, Buser AS, Teo SS, Tiedt R, Passweg JR, et al. A gain-of-function mutation of JAK2 in myeloproliferative disorders. N Engl J Med 2005;352:1779–90.
[22] Saharinen P, Takaluoma K, Silvennoinen O. Regulation of the Jak2 tyrosine kinase by its pseudokinase domain. Mol Cell Biol 2000;20:3387–95.
[23] Argetsinger LS, Kouadio JL, Steen H, Stensballe A, Jensen ON, Carter-Su C. Autophosphorylation of JAK2 on tyrosines 221 and 570 regulates its activity. Mol Cell Biol 2004;24:4955–67.

Oncogene (2007) 26, 1245–1255

www.nature.com/onc

ONCOGENOMICS

A genomic analysis of adult T-cell leukemia

YL Choi[1], K Tsukasaki[2], MC O'Neill[3], Y Yamada[4], Y Onimaru[2], K Matsumoto[5], J Ohashi[6], Y Yamashita[1], S Tsutsumi[7], R Kaneda[1], S Takada[1], H Aburatani[7], S Kamihira[4], T Nakamura[5], M Tomonaga[2] and H Mano[1,8]

[1]Division of Functional Genomics, Jichi Medical University, Shimotsukeshi, Tochigi, Japan; [2]Atomic Bomb Disease Institute, Nagasaki University Graduate School of Biomedical Science, Nagasaki, Japan; [3]Department of Biological Sciences, University of Maryland, Baltimore, MD, USA; [4]Department of Laboratory Medicine, Nagasaki University Graduate School of Biomedical Science, Nagasaki, Japan; [5]Division of Molecular Regenerative Medicine, Osaka University Graduate School of Medicine, Osaka, Japan; [6]Department of Human Genetics, Graduate School of Medicine, University of Tokyo, Tokyo, Japan; [7]Research Center for Advanced Science and Technology, University of Tokyo, Tokyo, Japan and [8]CREST, Japan Science and Technology Agency, Saitama, Japan

Adult T-cell leukemia (ATL) is an intractable malignancy of CD4$^+$ T cells that is etiologically associated with infection by human T-cell leukemia virus-type I. Most individuals in the chronic stage of ATL eventually undergo progression to a highly aggressive acute stage. To clarify the mechanism responsible for this stage progression, we isolated CD4$^+$ cells from individuals in the chronic ($n=19$) or acute ($n=22$) stages of ATL and subjected them to profiling of gene expression with DNA microarrays containing >44 000 probe sets. Changes in chromosome copy number were also examined for 24 cell specimens with the use of microarrays harboring ~50 000 probe sets. Stage-dependent changes in gene expression profile and chromosome copy number were apparent. Furthermore, expression of the gene for MET, a receptor tyrosine kinase for hepatocyte growth factor (HGF), was shown to be specific to the acute stage of ATL, and the plasma concentration of HGF was increased in individuals in either the acute or chronic stage. HGF induced proliferation of a MET-positive ATL cell line, and this effect was blocked by antibodies to HGF. The HGF-MET signaling pathway is thus a potential therapeutic target for ATL.
Oncogene (2007) **26,** 1245–1255. doi:10.1038/sj.onc.1209898; published online 14 August 2006

Keywords: adult T-cell leukemia; DNA microarray; MET; artificial neural network

Introduction

Adult T-cell leukemia (ATL) is an intractable malignancy of CD4$^+$ T cells that is etiologically associated with infection by human T-cell leukemia virus-type I (HTLV-I) (Uchiyama *et al.*, 1977; Poiesz *et al.*, 1980; Yoshida *et al.*, 1982). Virally encoded proteins such as Tax trigger polyclonal growth of T cells in infected individuals, and there are an estimated 15–20 million such carriers worldwide (Edlich *et al.*, 2000). After a latency period of decades, a small proportion of carriers (~2%) develop ATL. Many ATL patients initially manifest only monoclonal (or oligoclonal) growth of leukemic clones without apparent clinical symptoms, a condition referred to as the chronic or smoldering stages (Shimoyama, 1991). Most individuals in the chronic stage, however, eventually undergo progression to a highly aggressive acute stage (Tajima, 1990). Given that the prognosis of individuals at the acute stage remains very poor, it is important to clarify the molecular mechanism that underlies stage progression.

Homozygous deletion or epigenetic silencing of the gene for the cyclin-dependent kinase inhibitor p16 (Hatta *et al.*, 1995; Yamada *et al.*, 1997; Nosaka *et al.*, 2000) as well as altered expression of other genes related to cell proliferation (Cesarman *et al.*, 1992; Tamiya *et al.*, 1998) have been detected in ATL cells at the acute stage. However, such genetic or epigenetic changes may be infrequent (Matsuoka, 2003), and the transforming events responsible for chronic to acute stage progression remain largely unknown.

DNA microarray analysis allows simultaneous comparison of the expression intensities of tens of thousands of genes. Such analysis of the transcriptomes of ATL cells at the chronic and acute stages might thus be expected to provide insight into the mechanism of stage progression in this disease. With the use of this approach, Sasaki *et al.* (2005) recently compared transcriptomes between normal CD4$^+$ T cells ($n=5$) and mononuclear cells (MNCs) isolated from individuals in the acute stage of ATL ($n=8$). Tsukasaki *et al.* (2004) also compared transcriptomes between MNCs from patients in the chronic or acute stages of ATL ($n=4$ for each). However, the significance of these data may be limited by the small number of study subjects and by the use of unfractionated MNCs that contain various proportions of non-ATL cells.

Correspondence: Dr H Mano, Division of Functional Genomics, Jichi Medical University, 3311-1 Yakushiji, Shimotsukeshi, Tochigi 329-0498, Japan.
E-mail: hmano@jichi.ac.jp
Received 20 March 2006; revised 10 July 2006; accepted 11 July 2006; published online 14 August 2006

In addition to changes in gene expression, ATL cells frequently manifest various karyotype anomalies. Comparative genomic hybridization (CGH) has thus revealed recurrent gains in chromosomes 2p, 3p, 7q and 14q as well as losses in 6q in ATL cells (Ariyama *et al.*, 1999; Tsukasaki *et al.*, 2001). However, CGH or its successor, bacterial artificial chromosome (BAC) array-based CGH, is able to analyse chromosome copy number alterations (CNAs) at a resolution of only several hundred kilobase pairs (Lockwood *et al.*, 2005). High-density oligonucleotide microarrays originally designed for genotyping of single nucleotide polymorphisms (SNPs) have recently been adapted for CNA analysis (Lin *et al.*, 2004; Nannya *et al.*, 2005). With this approach, chromosome copy number is inferred from the signal intensity of SNP probe sets distributed throughout the human genome. For instance, with Affymetrix GeneChip Mapping 100K arrays developed for genotyping of ~100 000 SNPs, it is possible to determine CNAs at a mean resolution of 23.6 kbp, which is substantially greater than that achievable with BAC array-based technologies.

With both microarray-based gene expression profiling and SNP array-based CNA profiling, we have now performed a comprehensive genomic analysis of ATL in order to investigate the mechanism of stage progression from chronic to acute. Given that the $CD4^+CD8^-$ fraction of peripheral blood (PB) cells of individuals with chronic or acute ATL is composed predominantly of ATL cells, we purified this fraction from ATL patients. We then subjected the isolated cells to gene expression profiling with microarrays containing >44 000 probe sets and to CNA analysis with microarrays harboring ~50 000 probe sets. The gene expression data indicate that the transcriptomes for the chronic and acute stages of ATL are distinct, and the CNA data reveal frequent amplification or deletion of genomic fragments of various sizes in each ATL stage.

Results

Transcriptomes of ATL cells

To characterize the transcriptomes of ATL cells, we purified $CD4^+$ cells from PB of ATL patients at either the chronic ($n=19$) or the acute ($n=22$) stage. The clinical characteristics of the patients are summarized in Supplementary Table 1. The $CD4^+$ fraction was also purified from healthy volunteers ($n=3$) and was either activated with phytohemagglutinin (PHA) or not.

A simple, one-step column purification with antibodies to CD4 yielded a highly pure $CD3^+CD4^+$ T-cell fraction. For example, whereas the $CD3^+CD4^+$ fraction constituted only 29.1% of PB MNCs of one healthy individual, it constituted 98.8% of the corresponding column eluate (Figure 1a). Similarly, $CD3^+CD4^+$ cells constituted 25.7% of MNCs from one ATL patient at the acute stage, but accounted for 97.5% of cells in the corresponding column eluate (data not shown).

All of the ATL and normal $CD4^+$ cell specimens were then subjected to expression profiling with ~44 000 probe sets (corresponding to ~33 000 transcripts) on Affymetrix HGU133 microarrays. To eliminate from the analysis genes that were transcriptionally silent in the ATL specimens, we first selected probe sets that received the 'Present' call by Microarray Suite 5.0 software (Affymetrix) in at least 30% ($n=13$) of the ATL samples. A total of 15 121 probe sets fulfilled this criterion. On the basis of the similarity of the expression profiles for these probe sets, all 47 samples were subjected to hierarchical two-way clustering (Alon *et al.*, 1999), yielding a dendrogram of the subjects (Figure 1b). All six normal samples, irrespective of PHA stimulation, formed a distinct branch separated from the ATL specimens, indicating that the overall gene expression profiles differed between normal and transformed T cells. However, samples corresponding to patients with chronic or acute ATL were not clearly separated from each other in this tree.

To compare the transcriptomes of ATL cells between chronic and acute stages, we conducted Student's *t*-test on the gene expression intensity for the 15 121 probe sets with the Benjamini and Hochberg false discovery rate (Reiner *et al.*, 2003) of 0.01, leading to the isolation of 84 probe sets (data not shown). To enrich probe sets whose expression level was high in at least one of the stages, we adopted another selection window, effect size (absolute difference in mean expression intensity) (Dhanasekaran *et al.*, 2001). We extensively compared the expression level of given probe sets determined by DNA microarray and by quantitative real-time reverse transcription–polymerase chain reaction (RT–PCR). With our normalization procedure (see Materials and methods), expression of genes with an array data of ⩾100 units (U) was almost always detected by real-time RT–PCR (data not shown). Thus, we chose 100 U as the threshold value for the effect size.

A total of 21 probe sets (corresponding to 21 independent genes) whose expression level contrasted the two clinical conditions were finally identified. Hierarchical two-way clustering analysis of the expression profiles of these stage-associated genes revealed that only two gene were preferentially expressed at the chronic stage, whereas the other 19 genes were preferentially expressed in the acute stage (Figure 1c and Supplementary Table 2). Interestingly, the latter gene cluster contains several genes encoding for growth-related proteins, such as nuclear receptor coactivator 3 (NCOA3, GenBank accession no. NM_006534), heat-shock 60-kDa protein 1 (HSPD1, GenBank accession no. NM_002156) and general transcription factor IIIA (GTF3A, GenBank accession no. BE542815).

Gene expression-based prediction of ATL stage

We next attempted to develop a microarray-based class prediction algorithm for ATL. Among several approaches examined, an artificial neural network (ANN) provided the highest accuracy for prediction (O'Neill and Song, 2003). ANNs are computer-based

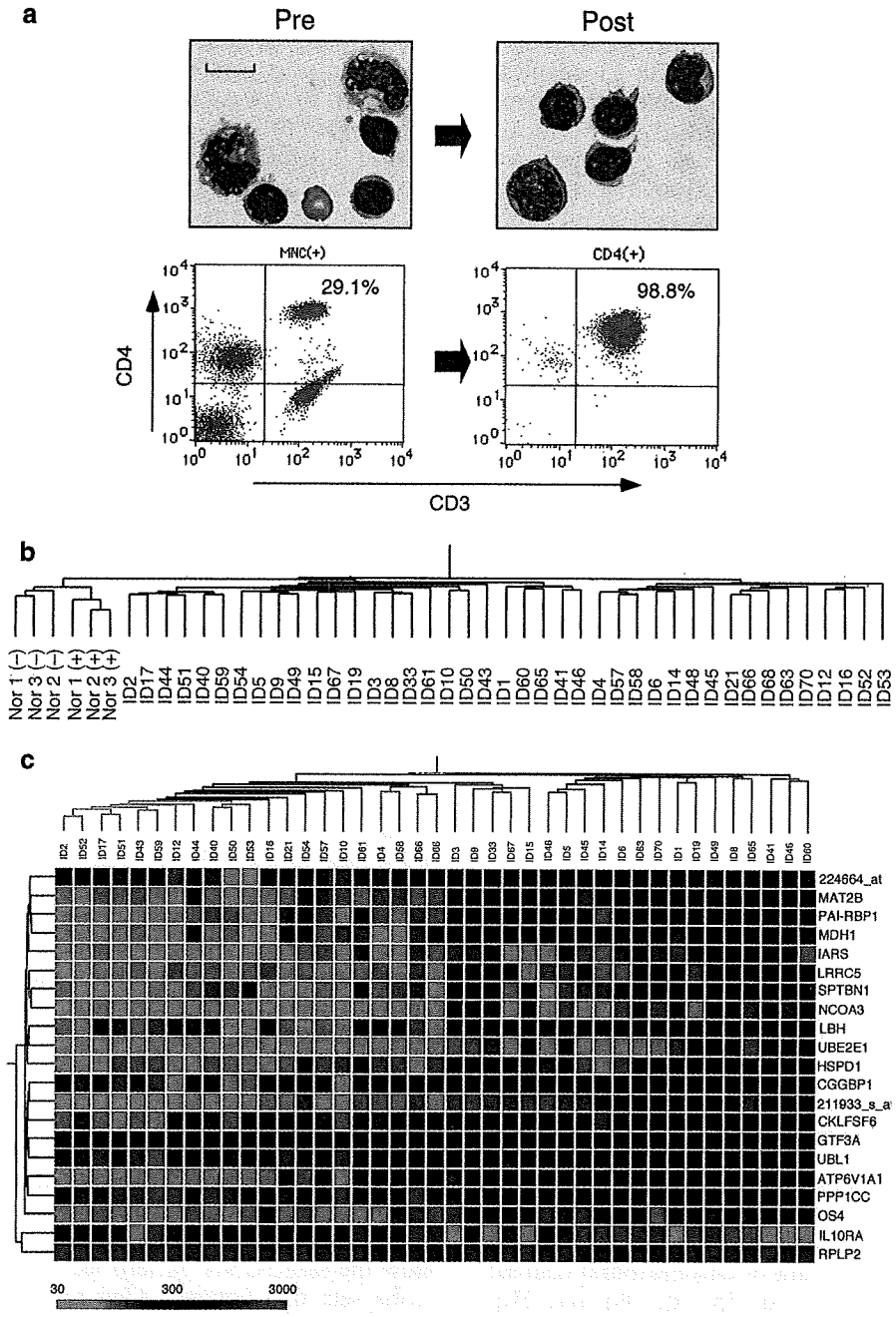

Figure 1 Purification and gene expression profiling of ATL cells. (**a**) MNCs isolated from the PB of a healthy individual were subjected to staining with Wright–Giemsa solution before (Pre) and after (Post) purification by affinity chromatography with antibodies to CD4 (upper panels). Scale bar, 10 μm. The same fractions were also subjected to flow cytometry with antibodies to CD3 and to CD4 (lower panels). The proportion of double-positive cells is indicated. (**b**) Subject tree generated by hierarchical clustering analysis of the expression profiles for 15 121 probe sets. Normal T cells (Nor 1–3) stimulated (+) or not (−) with PHA (8 μg/ml) clustered together, separate from the ATL samples from patients in the chronic (green) or acute (red) stage. (**c**) Subject tree generated by two-way clustering analysis with 21 probe sets that contrasted the two clinical conditions (Student's *t*-test with the Benjamini and Hochberg false discovery rate of 0.01, and effect size of $\geqslant$100 U). Each column corresponds to a separate sample, and each row to a probe set whose expression is color-coded according to the indicated scale. Gene symbols are shown on the right; 224664_at and 211933_s_at are the expressed sequence tag IDs designated by Affymetrix (http://www.affymetrix.com). Annotations and expression intensities for the probe sets are presented in Supplementary Table 2.

algorithms modeled on the structure and behavior of neurons in human brain. Pattern recognition by ANNs is accomplished by training the networks for multiple times in a supervised mode. ANNs adjust continuously their internal weighted connections to reduce the observed errors in matching input to output.

Here, the 15 121 probe sets originally selected in Figure 1b were divided into three nonoverlapping

groups, each of which was used as the input for 10 ANNs (Figure 2a). We performed a 10% crossvalidation rotation with 37 samples, training with 33 samples and testing of the remaining four samples. We then reduced the weight of one input in the first layer (one at a time by 15%), and the network was run again to evaluate the difference in the result from the original output. The same procedure was performed in turn for every input, in order to identify 44 'predictor' genes whose expression markedly influenced the prediction accuracy in each set of ANNs (Figure 2b and Supplementary Table 3). Such predictor set contains only one gene (*UBE2E1*) shared with the stage-associated probe sets shown in Figure 1c. As demonstrated previously, ANN and other approaches (such as *t*-test or clustering analysis) frequently isolate distinct sets of predictor genes (O'Neill and Song, 2003).

Another nine ANNs were then trained and tested with the 44 predictor genes in the same 10% crossvalidation round, yielding one error of prediction for the 37 samples. Finally, the withheld four samples were tested with the trained ANN, resulting in the correct prediction of the class of each. Given that diagnosis of the stage of ATL patients is sometimes problematic, especially when an individual is undergoing stage transition, our analysis offers the possibility of a microarray diagnostic system based on the expression profile of a small number of genes.

Copy number analysis of the ATL genome

To analyse chromosomal gain or loss in ATL cells, we subjected genomic DNA to hybridization with genotyping arrays that represent ~50 000 human SNPs and allow determination of copy number at an average resolution of 47.2 kbp. We first examined whether MNCs and purified $CD4^+$ ATL cells may yield similar CNA profiles by analyzing genomic DNA from such cell fractions of a single individual (patient ID6) at the acute stage of ATL. Flow cytometry revealed that $CD3^+CD4^+$ T cells constituted 58.9 and 98.0% of MNCs and purified $CD4^+$ cells of this individual, respectively (data not shown).

As shown in Figure 3a, gain of chromosomal content ($\geqslant 3n$) was apparent at 1q, 3q, 5p, 7q, 18q and 21q, whereas loss of genomic content ($\leqslant 1n$) was observed at 2p, 12p, 13q, 14q and 18p. In addition to changes affecting such large chromosomal regions, numerous CNAs too small to be detected by conventional methods were apparent at various positions (hospital karyotyping of MNCs from this patient indicated a karyotype of 46,XY). We also identified many chromosomal regions whose copy number differed between the unfractionated MNCs and purified $CD4^+$ cells (Figure 3a). These data indicate that purification of $CD4^+$ cells increases the sensitivity of copy number measurement.

Among the ATL specimens subjected to gene expression profiling, all those for which $CD4^+$ cells were available for preparation of genomic DNA were analysed for CNAs ($n=24$; 15 specimens for the acute stage, nine specimens for the chronic stage). Assessment of copy number revealed frequent anomalies of various sizes, ranging from amplification of an entire chromosome to small deletions spanning only a few probe sets, in the ATL genome (Figure 3b). The most frequent gain or loss in our data set was a small deletion at 14q11.2, which was identified in 22 of the 24 patients tested; the core deleted region spans five probe sets, encompassing as little as 30 857 bp at the locus of *TRD* (encoding T-cell receptor delta locus) and *TRA* (encoding T-cell receptor alpha constant). These deletions likely reflect genomic rearrangement at the T-cell receptor locus in ATL cells and support the high sensitivity of the method.

Further, a high-grade amplification of genome could be found in a region spanning ~14 Mbp at 3p (nucleotide 10 672 576–24 556 563) among the ATL patients, especially at the acute stage. A chromosome copy number of four in this region was inferred for three patients at the acute stage (ID 3, 15 and 70), and that of three was inferred for seven patients. Interestingly, expression level of the genes mapped on this 3p region was significantly higher in the patients with a chromosome copy number of four compared to those with a copy number of two ($P=0.03$, Student's *t*-test), and marginally higher to those with a copy number of three ($P=0.051$) (data not shown).

To confirm the inferred copy numbers in our data set, we subjected genomic DNA at a locus with marked variation in copy number (chromosome 6, nucleotides 16 651 304–16 651 533) to quantitative real-time PCR analysis. Such analysis of the 24 patients, two healthy volunteers (one male, one female), and a cell line (KK-1) (Imaizumi *et al*., 2003) derived from a patient at the acute stage of ATL revealed that the inferred copy number was highly correlated with DNA content measured by PCR (Figure 3c).

Stage-dependent CNAs

To screen for CNA patterns linked to stage progression in ATL, we applied Student's *t*-test ($P<0.01$) to the obtained data set. Subsequent application of a selection window specifying that at least two contiguous probes show the same CNA pattern led to the isolation of 330 probe sets that corresponded to 3p, 3q, 14q and 19p (Figure 3d). Segmental amplification of chromosome 3 was detected only in the ATL patients at the acute stage, consistent with previous results obtained by CGH analysis (Tsukasaki *et al*., 2001; Oshiro *et al*., 2006).

To examine the effect of gene dosage on mRNA abundance, we analysed our gene expression data set for the expression level of genes assigned to a segment (region #1, nucleotides 114 092 369–119 769 881) of chromosome 3 (Figure 3d and e). The mean expression intensity of genes in this region was significantly greater for the patients with a corresponding gain of DNA content than for those without such a gain ($P=0.00015$, Student's *t*-test). Similarly, the expression level of genes on a segment (region #2; nucleotide 8 782 486–12 322 072) of chromosome 19 was greater in cells with a gain of DNA content in this region than in those

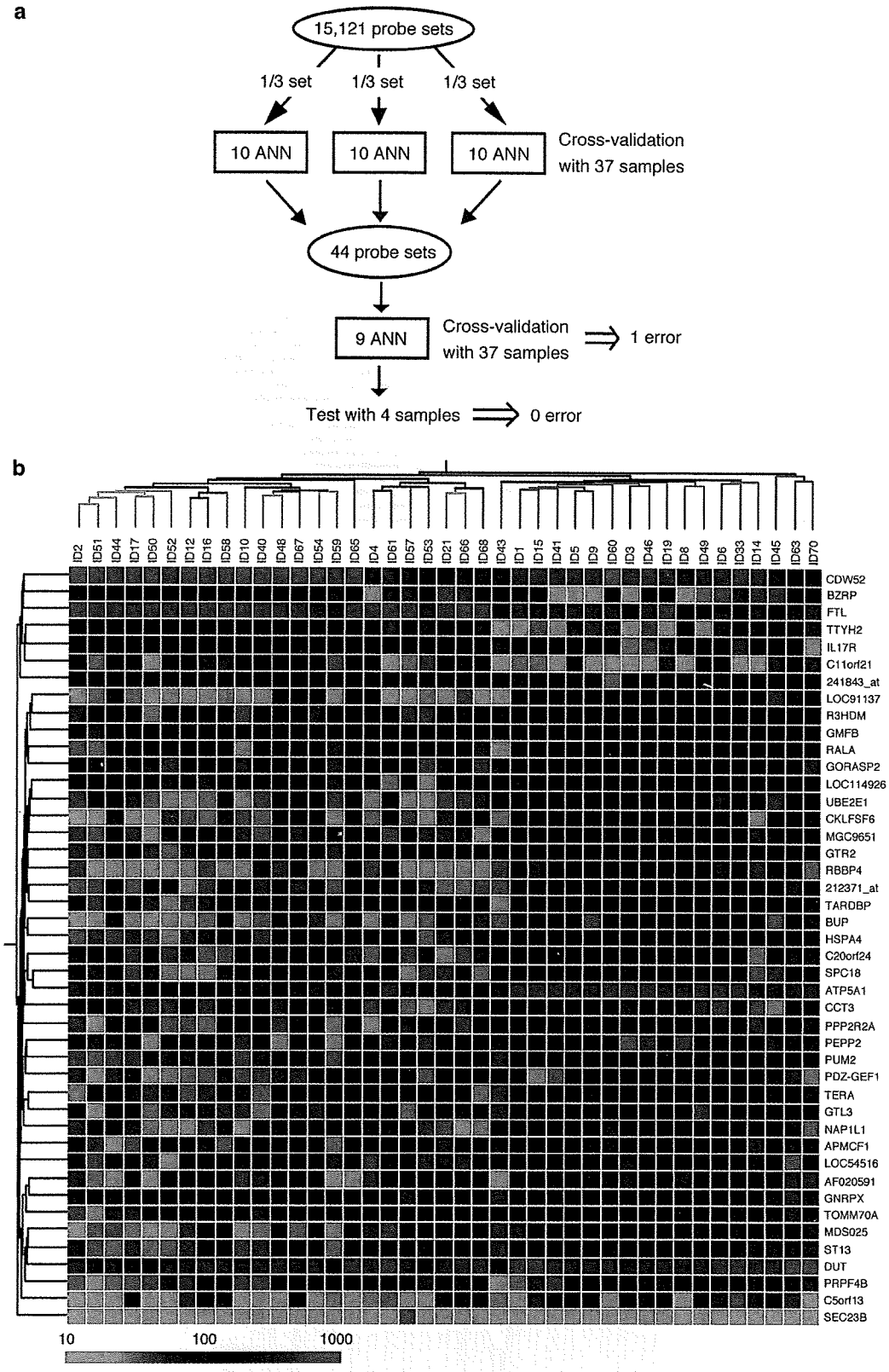

Figure 2 Schematic of the ANN analysis used for class prediction of ATL. **(a)** The 15 121 probe sets originally selected in Figure 1b were divided into three nonoverlapping groups, each of which was used as the input for 10 ANNs. We performed a 10% crossvalidation rotation with 37 samples, training with 33 samples and testing of the remaining four samples. On the basis of the differentiation process with the three sets of 10 ANNs, we selected 44 'predictor' genes whose expression markedly influenced the prediction accuracy in each set of ANNs. **(b)** Subject tree generated by two-way clustering analysis with the 44 predictor genes selected in **(a)** is demonstrated as in Figure 1c. 241843_at and 212371_at are the expressed sequence tag IDs designated by Affymetrix. Annotations and expression intensities for the probe sets are presented in Supplementary Table 3.

without such a gain ($P=0.0357$). These data indicate that gene dosage indeed affects transcript abundance in ATL cells. The large standard deviations apparent in the data shown in Figure 3e, however, suggest that other mechanisms (mediated by transcription factors or epigenetic regulation, for example) have also a large impact on gene expression level.

The hepatocyte growth factor-MET pathway in ATL cells

The long latency period for ATL in HTLV-I carriers suggests that the molecular pathogenesis of ATL and its stage progression might be highly heterogeneous. To identify molecular events that might contribute to transition to the acute stage, we next attempted to isolate 'acute stage-specific genes,' defined by their

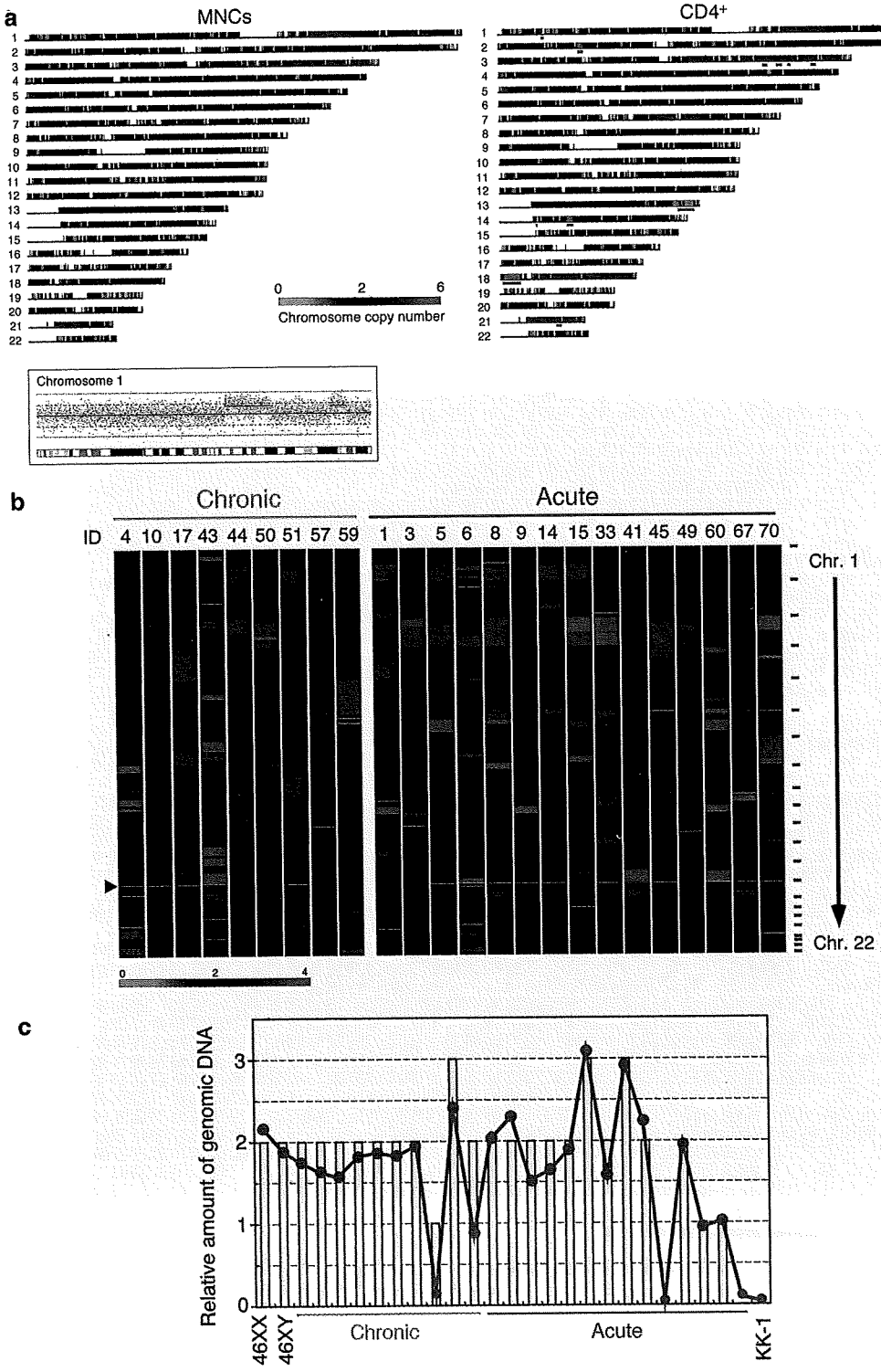

Figure 3 *Continued.*

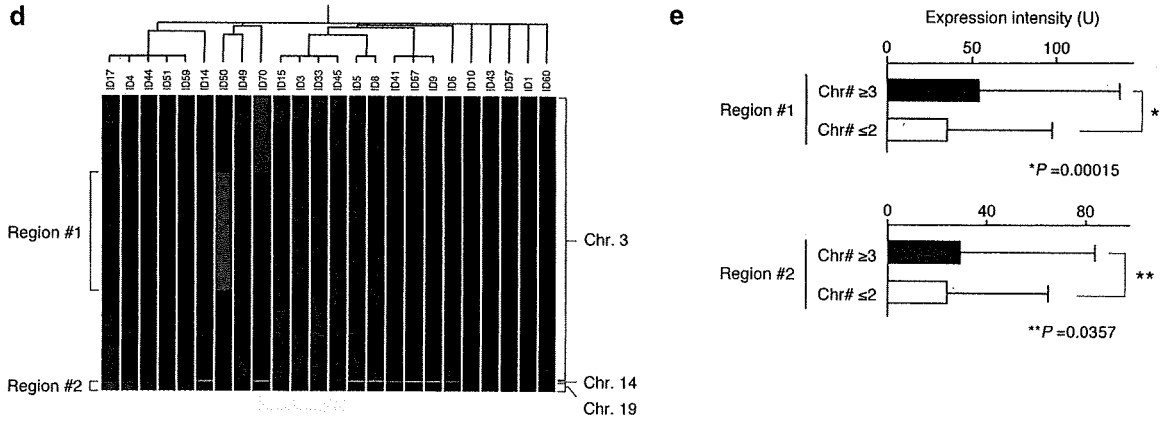

Figure 3 CNA analysis of purified ATL cells. (**a**) Inferred copy number for all SNP sites analysed in MNCs (left) and CD4+ cells (right) isolated from an ATL patient in the acute stage (ID6). Copy number is color-coded according to the indicated scheme. Chromosomal regions with an aberrant copy number detected only in CD4+ cells are indicated by blue underlines. An inset below demonstrates the raw signal ($\log_2$ ratio) for every SNP locus by the array hybridization (red dots) and corresponding inferred copy number (green lines) on chromosome 1 for the MNC sample, along with the chromosome cytobands. (**b**) Inferred copy number for all SNP sites (chromosomes 1–22) in all subjects studied ($n=9$ for chronic stage, $n=15$ for acute stage) shown according to the color scheme at the bottom. SNP sites are ordered by their physical position from top to bottom (shown on the right), and the borders between chromosomes are indicated by small bars. The most frequently deleted region at 14q11.2 is indicated by the arrowhead. (**c**) Inferred copy number (yellow columns) for a region of chromosome 6 (nucleotides 16 651 304–16 651 533) compared with the relative amount (blue line) of genomic DNA corresponding to this region (expressed relative to the amount of *GAPDH* genomic DNA). An ATL cell line (KK-1) and CD4+ cells isolated from a male (46XY) or female (46XX) volunteer were also analysed. (**d**) Subject tree based on inferred copy number of chromosomal regions that showed a statistically significant difference in copy number for at least two consecutive SNP sites between the acute and chronic stages of ATL ($P<0.01$, Student's *t*-test). (**e**) Comparison of expression intensities of the genes assigned to two chromosomal regions (region #1 and region #2) indicated in (**d**) between the subjects with or without a gain in chromosome copy number (Chr#) for the corresponding region. Data are means + s.d. The *P*-values were calculated by Student's *t*-test.

silence (expression level of <10 U) in all normal T cells and chronic ATL specimens and their activation (>100 U) in at least one of the acute-stage samples. We isolated six probe sets that fulfilled such criteria (Figure 4a and Supplementary Table 4).

Among these acute stage-specific genes, we focused on *MET* (GenBank accession no. NM_000245), given that we recently found, in an independent study, that the amount of *MET* mRNA was specifically increased in ATL cells that manifested liver invasion (Imaizumi *et al.*, 2003). *MET* encodes a transmembrane protein tyrosine kinase that is the receptor for hepatocyte growth factor (HGF) (Bottaro *et al.*, 1991). The expression level of *MET* in the study specimens as determined by microarray analysis was highly correlated with that determined by quantitative RT–PCR analysis (Figure 4b), as revealed by a Pearson's correlation coefficient (r) of 0.851 ($P<0.001$). (Also see Supplementary Table 5 for verification of microarray data by RT–PCR.) Flow cytometry revealed that the expression of MET at the cell surface reflected the abundance of the corresponding mRNA in ATL samples (Figure 4c).

The acute stage-specific expression of MET at both the mRNA and protein levels suggested that ATL cells might acquire mitogenic potential as a result of activation of a MET-linked signaling pathway. To examine the possible operation of an HGF-MET autocrine loop, we quantitated HGF mRNA in ATL cells by both microarray and quantitative RT–PCR analyses. No substantial amounts of HGF mRNA were detected in ATL specimens, however (data not shown).

We therefore next measured the plasma concentration of HGF in the study subjects. High levels of HGF were detected in the plasma of ATL patients, especially in that of individuals in the acute stage (Figure 5a), compared with the previously determined values for healthy adults (0.27 ± 0.08 ng/ml, mean ± s.d.) and some cancer patients (1–2 ng/ml) (Funakoshi and Nakamura, 2003). To test directly whether activation of the HGF-MET signaling pathway is able to promote the proliferation of ATL cells, we examined the MET-positive ATL cell line KK-1. HGF induced both the tyrosine phosphorylation of MET and proliferation in KK-1 cells (Figure 5b and c). The addition of antibodies to HGF (Montesano *et al.*, 1991) could abolish both effects.

Discussion

We have analysed gene expression and CNA profiles in leukemic cell-enriched fractions of individuals with ATL. We found that both types of profile differ markedly between the chronic and acute stages of ATL, and that the level of gene expression is influenced by the copy number of genomic DNA in ATL cells. Although ATL cells have previously been shown to manifest multiple genomic gains or losses (Ariyama *et al.*, 1999; Tsukasaki *et al.*, 2001), our data have revealed that the ATL genome is more unstable than has been appreciated. Similar complex CNAs have been identified by SNP array-based methods for other types

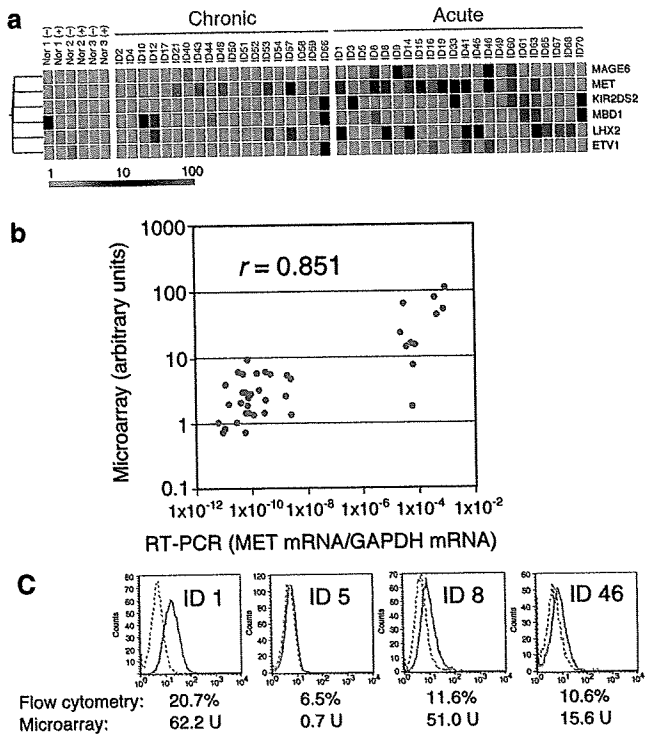

Figure 4 Acute stage-specific expression of *MET* in ATL. (**a**) Expression profiles of the six acute stage-specific probe sets. The expression level of each probe set is colored according to the indicated scale. Annotations and expression intensities for the probe sets are presented in Supplementary Table 4. (**b**) Comparison of the abundance of *MET* mRNA in the study specimens as determined by microarray and RT–PCR analyses. For the latter, the amount of *MET* mRNA is expressed relative to that of *GAPDH* mRNA. Pearson's correlation coefficient (r) for the comparison is indicated. (**c**) Cell surface expression of MET was examined by flow cytometry in four ATL samples corresponding to the acute stage. The solid and dashed traces were obtained with antibodies to MET and control antibodies, respectively. The proportion of MET$^+$ cells determined by flow cytometry is indicated together with the corresponding amount of *MET* mRNA determined by microarray analysis.

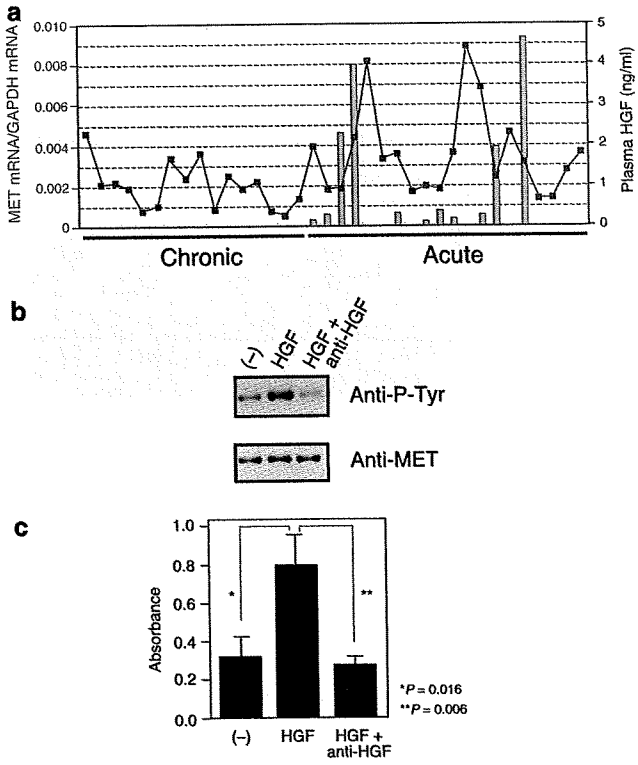

Figure 5 HGF-MET activity induces proliferation in ATL cells. (**a**) Comparison of the plasma concentration of HGF in ATL patients (as measured by enzyme-linked immunosorbent assay) with the corresponding amount of *MET* mRNA in leukemic cells (as determined by RT–PCR). (**b**) Tyrosine phosphorylation of MET in KK-1 cells incubated for 10 min in the absence (–) or presence of human HGF (50 ng/ml), alone or together with antibodies to HGF (10 μg/ml), was examined by immunoblot analysis of cell lysates with antibodies to phosphotyrosine (Anti-P-Tyr). The blot was also probed with antibodies to MET. (**c**) The proliferation of KK-1 cells (3×10^4) incubated for 1 day in the absence (–) or presence of HGF (50 ng/ml), alone or together with antibodies to HGF (10 μg/ml), was evaluated by the MTS assay. Data are expressed in absorbance units and are means + s.d. of triplicates from a representative experiment. The P-values for the indicated comparisons were determined by Student's t-test.

of cancer (Zhao *et al.*, 2005). We detected 3386.9 ± 2254.0 (mean $\pm$ s.d.) and 4678.5 ± 2874.6 SNP sites showing $\geqslant 3n$ ploidy as well as 1039.9 ± 2310.0 and 927.1 ± 1137.9 SNP sites with $\leqslant 1n$ ploidy in samples corresponding to the chronic and acute stages of ATL, respectively. The numbers of probe sets showing gain or loss of DNA content did not differ significantly ($P > 0.05$) between the chronic and acute stages of ATL. Given the large numbers of probe sets with an aberrant DNA content in the ATL genome, a large-scale study will likely be required to pinpoint the *bona fide* disease-dependent or stage-dependent CNAs.

Recently, with the use of BAC array-based CGH (with a mean resolution of 1.3 Mbp), Oshiro *et al.* (2006) have compared CNA of MNCs for 17 patients at the acute stage of ATL to that of lymph nodes for 42 cases with the lymphoma type of ATL. The recurrent gain of chromosomes was found at 3/3p among individuals with the acute stage of ATL, which is in good agreement with our results.

We found that an increased plasma concentration of HGF coexists with an increased expression of MET in ATL cells from some individuals at the acute stage of the disease. Together with the demonstrated mitogenic effect of HGF in ATL cells, these data suggest a novel scenario for stage progression in ATL. The mechanism responsible for the increased plasma level of HGF in ATL patients is unclear. Given that ATL is a malignancy of activated mature T cells, the leukemic cells secrete a variety of cytokines, including tumor necrosis factor-α and interleukin-1β (Wano *et al.*, 1987; Yamada *et al.*, 1996). Both of these cytokines are potent inducers of HGF expression in fibroblasts (Matsumoto *et al.*, 1992; Tamura *et al.*, 1993), suggesting that ATL cells may indirectly increase the plasma HGF level through secretion of these cytokines and consequent activation of fibroblasts.

Our data indicate that the plasma concentration of HGF in ATL patients increases before the onset of

expression of *MET* in the leukemic cells (Figure 5a). The increased concentration of HGF might therefore confer a growth advantage on ATL cells after they upregulate the expression of MET. Given that the JAK-STAT signaling pathway is activated in the leukemic cells of patients with advanced ATL (Migone *et al.*, 1995), it may be relevant that binding sites for STAT1 or STAT3 are present in the promoter regions of five (including *MET*) of the six acute stage-specific genes identified in the present study (Figure 4a). We did not detect a significant difference in DNA content (in our data set) for the *MET* locus between chronic and acute stages of ATL. It is thus possible that JAK-STAT signaling contributes to transcriptional activation of *MET*.

Given that our data are derived from purified ATL cells, they can be further used to characterize ATL in various ways. For instance, we attempted to isolate genes whose expression was linked to the presence of hypercalcemia in the study patients (data not shown); such genes included that for parathyroid hormone-like hormone (GenBank accession no. BC005961), which has been shown to be responsible for many instances of humoral hypercalcemia in individuals with cancer including ATL (Broadus *et al.*, 1988; Motokura *et al.*, 1988).

We have demonstrated the existence of an HGF-MET paracrine loop specific to the acute stage of ATL. Given that ligation of MET by HGF promoted the proliferation of ATL cells, activation of the HGF-MET signaling pathway is a candidate molecular mechanism for stage progression in ATL. Furthermore, our observation that this mitogenic effect was blocked by antibodies to HGF provides potential new targets for ATL therapy.

Materials and methods

Expression profiling

All clinical specimens were obtained with written informed consent, and the study was approved by the ethics committees of both Jichi Medical University and Nagasaki University. The diagnosis of ATL in all cases was based on clinical features, immunophenotypes of leukemic cells, and the monoclonal integration of HTLV-1 proviral DNA into the genome of leukemic cells (Shimoyama, 1991). MNCs isolated from PB were labeled with magnetic bead-conjugated mouse monoclonal antibodies to CD4 (CD4 MicroBeads, Miltenyi Biotec, Auburn, CA, USA). For PHA stimulation, purified $CD4^+$ cells from healthy individuals were incubated for 48 h in Rosewell's Park Memorial Institute media (RPMI) 1640 medium (Invitrogen, Carlsbad, CA, USA) supplemented with 10% fetal bovine serum (FBS) and PHA-P (8 μg/ml) (Sigma, St Louis, MO, USA).

Column fractionation of MNCs, RNA preparation, and hybridization with HGU133A & B microarrays (Affymetrix, Santa Clara, CA, USA) were performed as described previously (Choi *et al.*, 2004). The mean expression intensity of the internal positive control probe sets (http://www.affymetrix.com/support/technical/mask_files.affx) was set to 500 U in each hybridization, and the fluorescence intensity of each test gene was normalized accordingly. All HGU133A & B microarray data are available at the Gene Expression Omnibus web site (http://www.ncbi.nlm.nih.gov/geo) under the accession number GSE1466.

Student's *t*-test with the Benjamini and Hochberg false discovery rate option was performed with GeneSpring 7.0 software (Silicon Genetics). Effect size was defined as an absolute difference in mean expression intensity between a given pair of classes (Dhanasekaran *et al.*, 2001). Education of and prediction by our ANN were performed with NeuralWorks Professional II Plus v.5.3 software (NeuralWare, Carnegie, PA, USA) as described previously (O'Neill and Song, 2003).

Analysis of CNA

Genomic DNA was obtained from purified $CD4^+$ ATL cells ($n=24$) and from MNCs of patient ID6 with the use of a QIAmp DNA Mini Kit (Qiagen, Valencia, CA, USA). Each DNA sample (250 ng) was digested with *Hind*III, ligated to Adaptor-Hind (Affymetrix), amplified by PCR, and subjected to hybridization with Mapping 50K Hind 240 arrays (Affymetrix). Chromosome copy number at each SNP site was inferred from hybridization signal intensity on the arrays with the use of CNAG software (http://www.genome.umin.jp) (Nannya *et al.*, 2005). For a normal reference, we used array data of PB MNCs isolated from four healthy volunteers. Assessment of copy number for all SNP sites is demonstrated in Supplementary Table 6. The raw data of Mapping 50K Hind 240 arrays is available upon request. Statistical analysis of copy number was performed with GeneSpring 7.0. Alterations in the amount of genomic DNA were confirmed by quantitative real-time PCR with an ABI PRISM 7700 sequence detection system (PE Applied Biosystems, Foster City, CA, USA). The oligonucleotide primers were 5′-AGCATGTCCACAAATGGCCTTTGG-3′ and 5′-CAGTTTTCCTGTCATGGGAAAGGG-3′ for a region of chromosome 6, and 5′-CTGACCTGCCGTCTA GAAAAACCT-3′ and 5′-CAGGAAATGAGCTTGACAA AGTGG-3′ for the glyceraldehyde-3-phosphate dehydrogenase (*GAPDH*) gene.

MET expression

ATL cells were stained with rabbit polyclonal antibodies to MET (Santa Cruz Biotechnology, Santa Cruz, CA, USA) or with mouse monoclonal antibodies to CD3 and to CD4 (both from BD Biosciences, San Diego, CA, USA) and were then subjected to flow cytometry with a FACScan instrument (BD Biosciences). The concentration of HGF in plasma was determined with a Quantikine ELISA kit for human HGF (R&D Systems, Minneapolis, MN, USA).

For quantitative RT–PCR analysis of *MET* expression, portions of nonamplified cDNA were subjected to PCR with a QuantiTect SYBR Green PCR kit (Qiagen). The oligonucleotide primers for PCR were 5′-GTCAGTGGTGGACCTG ACCT-3′ and 5′-TGAGCTTGACAAAGTGGTCG-3′ for *GAPDH* cDNA, and 5′-ACTTGTTGCAAGGGAGAAGAC TCC-3′ and 5′-AGCGTTCACATGGACATAGTGCTC-3′ for *MET* cDNA.

KK-1 cell experiments

KK-1 cells were maintained in RPMI 1640 medium supplemented with 10% FBS and recombinant human interleukin-2 (10 ng/ml) (Sigma). For immunoblot analysis, cells were cultured for 48 h without FBS and interleukin-2 and then incubated for 10 min with recombinant human HGF (50 ng/ml) (Sigma) either alone or together with rabbit polyclonal antibodies to HGF (10 μg/ml) (Montesano *et al.*, 1991). The

cells were then lysed and subjected to immunoblot analysis with mouse monoclonal antibodies to phosphotyrosine (4G10, Upstate Biotechnology, Charlottesville, VA, USA) or with rabbit polyclonal antibodies to MET (#05–237, Upstate Biotechnology) as described previously (Yamashita *et al.*, 2001). For assay of cell proliferation, serum-deprived KK-1 cells were cultured for 24 h at a density of 5×10^5/ml with HGF (50 ng/ml) either alone or together with antibodies to HGF (10 μg/ml) and were then mixed with MTS [3-(4,5-dimethylthiazol-2-yl)-5-(3-carboxymethoxyphenyl)-2-(4-sulfophenyl)-2*H*-tetrazolium, inner salt]. Cell proliferation was measured with a CellTiter 96 Aqueous One Solution Cell Proliferation Assay (Promega, Madison, WI, USA).

Abbreviations

ATL, Adult T-cell leukemia; PCR, polymerase chain reaction; PHA, phytohemagglutinin; ANN, artificial neural network; CNA, copy number alterations; HGF, hepatocyte growth factor.

Acknowledgements

This study was supported in-part by a grant for Third-Term Comprehensive Control Research for Cancer from the Ministry of Health, Labor and Welfare of Japan, and by a grant for Scientific Research on Priority Areas 'Applied Genomics' from the Ministry of Education, Culture, Sports, Science and Technology of Japan.

References

Alon U, Barkai N, Notterman DA, Gish K, Ybarra S, Mack D *et al.* (1999). Broad patterns of gene expression revealed by clustering analysis of tumor and normal colon tissues probed by oligonucleotide arrays. *Proc Natl Acad Sci USA* **96**: 6745–6750.

Ariyama Y, Mori T, Shinomiya T, Sakabe T, Fukuda Y, Kanamaru A *et al.* (1999). Chromosomal imbalances in adult T-cell leukemia revealed by comparative genomic hybridization: gains at 14q32 and 2p16–22 in cell lines. *J Hum Genet* **44**: 357–363.

Bottaro DP, Rubin JS, Faletto DL, Chan AM, Kmiecik TE, Vande Woude GF *et al.* (1991). Identification of the hepatocyte growth factor receptor as the c-met proto-oncogene product. *Science* **251**: 802–804.

Broadus AE, Mangin M, Ikeda K, Insogna KL, Weir EC, Burtis WJ *et al.* (1988). Humoral hypercalcemia of cancer. Identification of a novel parathyroid hormone-like peptide. *N Engl J Med* **319**: 556–563.

Cesarman E, Chadburn A, Inghirami G, Gaidano G, Knowles DM. (1992). Structural and functional analysis of oncogenes and tumor suppressor genes in adult T-cell leukemia/lymphoma shows frequent p53 mutations. *Blood* **80**: 3205–3216.

Choi YL, Makishima H, Ohashi J, Yamashita Y, Ohki R, Koinuma K *et al.* (2004). DNA microarray analysis of natural killer cell-type lymphoproliferative disease of granular lymphocytes with purified CD3(−)CD56(+) fractions. *Leukemia* **18**: 556–565.

Dhanasekaran SM, Barrette TR, Ghosh D, Shah R, Varambally S, Kurachi K *et al.* (2001). Delineation of prognostic biomarkers in prostate cancer. *Nature* **412**: 822–826.

Edlich RF, Arnette JA, Williams FM. (2000). Global epidemic of human T-cell lymphotropic virus type-I (HTLV-I). *J Emerg Med* **18**: 109–119.

Funakoshi H, Nakamura T. (2003). Hepatocyte growth factor: from diagnosis to clinical applications. *Clin Chim Acta* **327**: 1–23.

Hatta Y, Hirama T, Miller CW, Yamada Y, Tomonaga M, Koeffler HP. (1995). Homozygous deletions of the p15 (MTS2) and p16 (CDKN2/MTS1) genes in adult T-cell leukemia. *Blood* **85**: 2699–2704.

Imaizumi Y, Murota H, Kanda S, Hishikawa Y, Koji T, Taguchi T *et al.* (2003). Expression of the c-Met proto-oncogene and its possible involvement in liver invasion in adult T-cell leukemia. *Clin Cancer Res* **9**: 181–187.

Lin M, Wei LJ, Sellers WR, Lieberfarb M, Wong WH, Li C. (2004). dChipSNP: significance curve and clustering of SNP-array-based loss-of-heterozygosity data. *Bioinformatics* **20**: 1233–1240.

Lockwood WW, Chari R, Chi B, Lam WL. (2005). Recent advances in array comparative genomic hybridization technologies and their applications in human genetics. *Eur J Hum Genet* **14**: 139–148.

Matsumoto K, Okazaki H, Nakamura T. (1992). Up-regulation of hepatocyte growth factor gene expression by interleukin-1 in human skin fibroblasts. *Biochem Biophys Res Commun* **188**: 235–243.

Matsuoka M. (2003). Human T-cell leukemia virus type I and adult T-cell leukemia. *Oncogene* **22**: 5131–5140.

Migone TS, Lin JX, Cereseto A, Mulloy JC, O'Shea JJ, Franchini G *et al.* (1995). Constitutively activated Jak-STAT pathway in T cells transformed with HTLV-I. *Science* **269**: 79–81.

Montesano R, Matsumoto K, Nakamura T, Orci L. (1991). Identification of a fibroblast-derived epithelial morphogen as hepatocyte growth factor. *Cell* **67**: 901–908.

Motokura T, Fukumoto S, Takahashi S, Watanabe T, Matsumoto T, Igarashi T *et al.* (1988). Expression of parathyroid hormone-related protein in a human T cell lymphotrophic virus type I-infected T cell line. *Biochem Biophys Res Commun* **154**: 1182–1188.

Nannya Y, Sanada M, Nakazaki K, Hosoya N, Wang L, Hangaishi A *et al.* (2005). A robust algorithm for copy number detection using high-density oligonucleotide single nucleotide polymorphism genotyping arrays. *Cancer Res* **65**: 6071–6079.

Nosaka K, Maeda M, Tamiya S, Sakai T, Mitsuya H, Matsuoka M. (2000). Increasing methylation of the CDKN2A gene is associated with the progression of adult T-cell leukemia. *Cancer Res* **60**: 1043–1048.

O'Neill MC, Song L. (2003). Neural network analysis of lymphoma microarray data: prognosis and diagnosis near-perfect. *BMC Bioinformatics* **4**: 13.

Oshiro A, Tagawa H, Ohshima K, Karube K, Uike N, Tashiro Y *et al.* (2006). Identification of subtype-specific genomic alterations in aggressive adult T-cell leukemia/lymphoma. *Blood* **107**: 4500–4507.

Poiesz BJ, Ruscetti FW, Gazdar AF, Bunn PA, Minna JD, Gallo RC. (1980). Detection and isolation of type C retrovirus particles from fresh and cultured lymphocytes of a patient with cutaneous T-cell lymphoma. *Proc Natl Acad Sci USA* **77**: 7415–7419.

Reiner A, Yekutieli D, Benjamini Y. (2003). Identifying differentially expressed genes using false discovery rate controlling procedures. *Bioinformatics* **19**: 368–375.

Sasaki H, Nishikata I, Shiraga T, Akamatsu E, Fukami T, Hidaka T *et al.* (2005). Overexpression of a cell adhesion molecule, TSLC1, as a possible molecular marker for acute-type adult T-cell leukemia. *Blood* **105**: 1204–1213.

Shimoyama M. (1991). Diagnostic criteria and classification of clinical subtypes of adult T-cell leukaemia-lymphoma. A report from the Lymphoma Study Group (1984–1987). *Br J Haematol* **79**: 428–437.

Tajima K. (1990). The 4th nation-wide study of adult T-cell leukemia/lymphoma (ATL) in Japan: estimates of risk of ATL and its geographical and clinical features. The T- and B-cell Malignancy Study Group. *Int J Cancer* **45**: 237–243.

Tamiya S, Etoh K, Suzushima H, Takatsuki K, Matsuoka M. (1998). Mutation of CD95 (Fas/Apo-1) gene in adult T-cell leukemia cells. *Blood* **91**: 3935–3942.

Tamura M, Arakaki N, Tsubouchi H, Takada H, Daikuhara Y. (1993). Enhancement of human hepatocyte growth factor production by interleukin-1 alpha and -1 beta and tumor necrosis factor-alpha by fibroblasts in culture. *J Biol Chem* **268**: 8140–8145.

Tsukasaki K, Krebs J, Nagai K, Tomonaga M, Koeffler HP, Bartram CR *et al.* (2001). Comparative genomic hybridization analysis in adult T-cell leukemia/lymphoma: correlation with clinical course. *Blood* **97**: 3875–3881.

Tsukasaki K, Tanosaki S, DeVos S, Hofmann WK, Wachsman W, Gombart AF *et al.* (2004). Identifying progression-associated genes in adult T-cell leukemia/lymphoma by using oligonucleotide microarrays. *Int J Cancer* **109**: 875–881.

Uchiyama T, Yodoi J, Sagawa K, Takatsuki K, Uchino H. (1977). Adult T-cell leukemia: clinical and hematologic features of 16 cases. *Blood* **50**: 481–492.

Wano Y, Hattori T, Matsuoka M, Takatsuki K, Chua AO, Gubler U *et al.* (1987). Interleukin 1 gene expression in adult T cell leukemia. *J Clin Invest* **80**: 911–916.

Yamada Y, Hatta Y, Murata K, Sugawara K, Ikeda S, Mine M *et al.* (1997). Deletions of p15 and/or p16 genes as a poor-prognosis factor in adult T-cell leukemia. *J Clin Oncol* **15**: 1778–1785.

Yamada Y, Ohmoto Y, Hata T, Yamamura M, Murata K, Tsukasaki K *et al.* (1996). Features of the cytokines secreted by adult T cell leukemia (ATL) cells. *Leuk Lymphoma* **21**: 443–447.

Yamashita Y, Kajigaya S, Yoshida K, Ueno S, Ota J, Ohmine K *et al.* (2001). Sak serine/threonine kinase acts as an effector of Tec tyrosine kinase. *J Biol Chem* **276**: 39012–39020.

Yoshida M, Miyoshi I, Hinuma Y. (1982). Isolation and characterization of retrovirus from cell lines of human adult T-cell leukemia and its implication in the disease. *Proc Natl Acad Sci USA* **79**: 2031–2035.

Zhao X, Weir BA, LaFramboise T, Lin M, Beroukhim R, Garraway L *et al.* (2005). Homozygous deletions and chromosome amplifications in human lung carcinomas revealed by single nucleotide polymorphism array analysis. *Cancer Res* **65**: 5561–5570.

Supplementary Information accompanies the paper on the Oncogene website (http://www.nature.com/onc).

Oncogene (2007) 26, 1256

www.nature.com/onc

ERRATUM

Imatinib enhances human melanoma cell susceptibility to TRAIL-induced cell death: relationship to Bcl-2 family and caspase activation

A Hamaï, C Richon, F Meslin, F Faure, A Kauffmann, Y Lecluse, A Jalil, L Larue, MF Avril, S Chouaib and M Mehrpour

Oncogene (2007) **26,** 1256. doi:10.1038/sj.onc.1210213

Correction to:
Oncogene (2006) **25**, 7618–7634. doi:10.1038/sj.onc.1209738; published online 18 September 2006

Due to a typesetting error, an incorrect version of figure 6d was published. The correct version of the figure is given here.

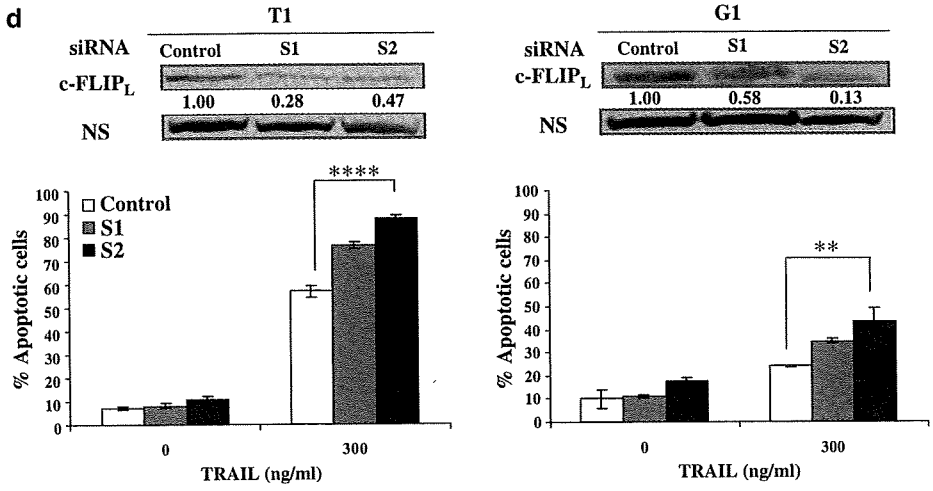

Available online at www.sciencedirect.com
ScienceDirect
ELSEVIER
Biochemical and Biophysical Research Communications 356 (2007) 723–726
BBRC
www.elsevier.com/locate/ybbrc

Transforming activity of purinergic receptor P2Y, G-protein coupled, 2 revealed by retroviral expression screening

Hisashi Hatanaka [a,b], Shuji Takada [a], Young Lim Choi [a], Shin-ichiro Fujiwara [a], Manabu Soda [a], Munehiro Enomoto [a], Kentaro Kurashina [a], Hideki Watanabe [a], Yoshihiro Yamashita [a], Kentaro Sugano [b], Hiroyuki Mano [a,c,*]

[a] *Division of Functional Genomics, Jichi Medical University, 3311-1 Yakushiji, Shimotsukeshi, Tochigi 329-0498, Japan*
[b] *Division of Gastroenterology, Jichi Medical University, Tochigi 329-0498, Japan*
[c] *CREST, Japan Science and Technology Agency, Saitama 332-0012, Japan*

Received 5 March 2007
Available online 19 March 2007

Abstract

Colorectal cancer (CRC) is one of the leading causes of cancer death in humans. In order to identify novel cancer-promoting genes in CRC, we here constructed a retroviral cDNA expression library from a CRC cell line RKO, and used it for a focus formation assay with mouse 3T3 fibroblasts, leading to the identification of 42 independent cDNAs. One of such cDNAs turned out to encode purinergic receptor P2Y, G-protein coupled, 2 (P2RY2). The oncogenic potential of P2RY2 was confirmed *in vitro* with the focus formation assay as well as soft agar-growth assay, and also *in vivo* with a tumorigenicity assay in nude mice. While our *P2RY2* cDNA encodes a protein with two amino-acid substitutions compared to the reported one, we have confirmed that the wild-type P2RY2 has a strong transforming potential as well. These results indicate an unexpected role of P2RY2 in the carcinogenesis of human cancers.

Keywords: Purinergic receptor; Oncogene; Colorectal carcinoma; cDNA library; Retrovirus

Colorectal cancer (CRC) is a common malignancy accounting for ~10% of all cancer deaths in United States [1]. In 1990, Feason and Vogelstein postulated a "multistep process" model for the development of CRC [2]. They demonstrated that germline and/or somatic gene mutations are required for malignant transformation of colonic epithelial cells, and that it is the accumulation of multigenetic mutations rather than their sequence that determines the biological behavior of the tumor. Although vast efforts have been used to isolate candidates for such oncogenes involved in CRC, we still have few therapeutic targets to treat this intractable disorder.

The focus formation assay with 3T3 or RAT1 fibroblasts has been extensively used to screen for transforming genes in various carcinomas [3]. In such screening, genomic DNA is isolated from cancer specimens and used to transfect 3T3 fibroblasts to obtain transformed cell foci. It should be noted, however, that, since expression of any genes in these experiments is driven by their own promoters/enhancers, oncogenes in CRC can exert their effects in 3T3 cells only when the promoter/enhancer regions of such genes are active in fibroblasts, which is not always guaranteed.

To ensure the sufficient expression of cDNAs in 3T3 cells, their transcription should be regulated by an exogenous promoter fragment. We have therefore constructed a retroviral cDNA expression library from a CRC cell line, which was used to infect 3T3 cells. In the preparation of cDNA library, we further took advantage of the SMART polymerase chain reaction (PCR) system (Clontech, Palo

* Corresponding author. Address: Division of Functional Genomics, Jichi Medical University, 3311-1 Yakushiji, Shimotsukeshi, Tochigi 329-0498, Japan. Fax: +81 285 44 7322.
E-mail address: hmano@jichi.ac.jp (H. Mano).

0006-291X/$ - see front matter © 2007 Elsevier Inc. All rights reserved.
doi:10.1016/j.bbrc.2007.03.048

Alto, CA), which preferentially amplifies full-length cDNAs. A focus formation assay with the library resulted in an identification of a transforming purinergic receptor P2Y, G-protein coupled, 2 (P2RY2) cDNA.

Materials and methods

Cell lines and culture. RKO, NIH 3T3, and BOSC23 packaging cell lines [4] were obtained from American Type Culture Collection, and maintained in Dulbecco's modified Eagle's medium (DMEM)-F12 (Invitrogen, Carlsbad, CA) supplemented with 10% fetal bovine serum (Invitrogen) and 2 mM L-glutamine.

Construction of retroviral cDNA expression library. Total RNA was extracted from RKO cells with the use of an RNeasy Mini column and RNase-free DNase (both from Qiagen, Valencia, CA), and a retrovirus library was constructed as described previously [5,6]. Briefly, the first-strand cDNA was synthesized by PowerScript reverse transcriptase, SMART IIA oligonucleotide, and CDS primer IIA (all from Clontech). Full-length cDNAs were then amplified for 15 cycles with 5′ PCR primer IIA according to the instructions of the SMART PCR cDNA synthesis kit (Clontech) except a substitution of LA *Taq* polymerase (Takara Bio, Shiga, Japan) for Advantage 2 DNA polymerase provided with the kit. Resultant cDNAs were blunt-ended by T4 DNA polymerase and ligated to the BstXI adaptor (Invitrogen). Unbound adaptors were removed through the cDNA size fractionation column (Invitrogen), and the cDNAs were finally ligated to the pMXS retroviral plasmid (a kind gift of Dr. T. Kitamura at Institute of Medical Science, University of Tokyo) [7]. The pMXS-cDNA plasmids were introduced into ElectroMax DH10B cells (Invitrogen) with electroporation. A cDNA to encode wild-type P2RY2 was generated based on our P2RY2 cDNA with the use of QuickChange Multi Site-Directed Mutagenesis kit (Stratagene, La Jolla, CA).

Focus formation assay. BOSC23 cells (1.8×10^6) were seeded into a 6-cm culture dish, cultured for 24 h, and then transfected with 2 μg of retroviral plasmids mixed with 0.5 μg of pGP plasmid (Takara Bio), 0.5 μg of pE-eco plasmid (Takara Bio), and 18 μl of Lipofectamine reagent (Invitrogen). Two days after the transfection, polybrene (Sigma, St. Louis, MI) was added to the culture supernatant at a concentration of 4 μg/ml, and the supernatant was subsequently used to infect 3T3 cells for 48 h. For the focus formation assay, culture medium of 3T3 cells was then changed to DMEM-F12 supplemented with 5% calf serum and 2 mM L-glutamine. Transformed foci were picked up after 3 weeks of culture. Genomic DNA was extracted from each transformed focus, and was subjected to PCR with 5′ PCR primer IIA (Clontech) and LA Taq polymerase for 40 cycles of 98 °C for 20 s and 68 °C for 6 min. Amplified genome fragments were purified after gel electrophoresis and ligated to pGEM-T Easy vector (Promega) for nucleotide sequencing.

Tumorigenicity assay in nude mice. 3T3 cells (2×10^6) were infected with a retrovirus encoding P2RY2, resuspended in 500 μl of phosphate-buffered saline, and injected into each shoulder of nu/nu Balb-c mouse (6 weeks old). Tumor formation was assessed after 3 weeks.

Anchorage-independent growth in soft agar. 3T3 cells (2×10^6) were infected with a retrovirus encoding P2RY2 or v-Ras, resuspended in the culture medium supplemented with 0.4% agar [Sea Plaque GTG agarose (Cambrex, East Rutherford, NJ)], and seeded onto a base layer of complete medium supplemented with 0.5% agar. Cell growth was assessed after culture for 2 weeks.

Results

Screening with focus formation assay

From mRNA of RKO cells, full-length cDNAs were selectively amplified and ligated to a retroviral vector pMXS. We could obtain a total of 2.5×10^6 colony forming units of independent plasmid clones. Thirty-nine clones were randomly isolated from the library and examined for the incorporated cDNAs. Thirty-seven (94.8%) out of the 39 clones contained inserts with an average length of 1.86 kbp.

By introducing the plasmid DNA into a packaging cell line, we generated a recombinant ecotropic retrovirus library that was subsequently used to infect mouse 3T3 fibroblasts. Infection experiments were repeated for a total of six times. After 3 weeks of culture, 50 transformed foci were observed. No foci could be found among the cells infected with an empty virus, while numerous foci were easily identified in the cells infected with a virus expressing v-Ras oncoprotein.

Each focus was isolated, expanded independently, and used to prepare genomic DNA. We then tried to recover retroviral inserts from such genomic DNA by PCR

Table 1
RKO cDNAs isolated from 3T3 transformants

Clone ID #	Gene symbol	GenBank No.	Presence of full ORF
1	*EIF5A*	NM_001970	Yes
2	*SQLE*	NM_003129	Yes
3	*APEH*	NM_001640	Yes
4	*C7orf20*	NM_015949	Yes
5	*WDR34*	NM_052844	ND
6	*ADRM1*	NM_007002	Yes
7	*C7orf20*	NM_015949	ND
8	*BSG*	NM_198589	Yes
9	*RRAS2*	NM_012250	Yes
10	*SNX3*	NM_152827	Yes
11	*RPUSD1*	NM_058192	Yes
12	*MRPS34*	NM_023936	Yes
13	*KIAA0192*	NM_014730	No
14	*H2AFZ*	NM_002106	Yes
15	*FLJ37562*	NM_152409	Yes
16	*ESRRA*	NM_004451	ND
17	*RPS2*	NM_002952	Yes
18	*YWHAB*	NM_139323	Yes
19	*DEGS1*	NM_003676	Yes
20	*VKORC1*	NM_024006	Yes
21	*PITX1*	NM_002653	No
22	*P2RY2*	NM_002564	Yes
23	*CD320*	NM_016579	ND
24	*SNX3*	NM_152828	Yes
25	*MKNK2*	NM_017572	Yes
26	*FLOT1*	NM_005803	ND
27	*KIAA0196*	NM_014846	No
28	*ARHGEF1*	NM_199002	Yes
29	*SCLY*	NM_016510	Yes
30	*ASH2L*	NM_004674	Yes
31	*IFRD2*	NM_006764	Yes
32	*PTGES2*	NM_025072	Yes
33	*SLC43A1*	NM_003627	Yes
34	*AKR7A2*	NM_003689	ND
35	*CD81*	NM_004356	ND
36	*ASB6*	NM_017873	Yes
37	*PRO1855*	NM_018509	ND
38	*PLEC1*	NM_201384	No
39	*HSPA14*	NM_016299	Yes
40	*IARS2*	NM_018060	Yes
41	*GPC1*	NM_002081	Yes
42	*TGFB1*	NM_000660	ND

ORF, open-reading frame; ND, not determined.

amplification with the primer used originally to amplify the cDNAs in the construction of the library. In most cases, two to three DNA fragments were recovered from each genome, implying a multiple retroviral infection on the recipient 3T3 cells.

We obtained a total of 78 cDNA fragments by PCR, each of which was ligated into a cloning vector, and subjected to nucleotide sequencing from both ends. Screening of the 78 cDNA sequences against the public nucleotide sequence databases revealed that the 78 fragments correspond to 42 independent genes (Table 1).

Identification of mutated P2RY2

To confirm the transforming potential of the isolated cDNAs, each cDNA clone was ligated to pMXS, and corresponding retrovirus was used to re-infect 3T3 cells. Focus formation assays were conducted for 22 independent genes, discovering a reproducible transforming activity for clone ID #9 corresponding to *RRAS2* (GenBank Accession No., NM_012250), clone ID #28 corresponding to *ARHGEF1* (GenBank Accession No., NM_0199002), and clone ID #22 corresponding to *P2RY2* (GenBank Accession No., NM_002564) (Fig. 1, top). We focus on *P2RY2* in this report.

The entire coding region of our ID #22 cDNA was sequenced, revealing two non-synonymous nucleotide changes compared to the published *P2RY2* cDNA sequence. One such change was that the "C" at nucleotide position 470 in the reported sequence is replaced with a "T" in our sequence, leading to the proline to leucine change at amino-acid position 46 (Fig. 2).

The other change was at nucleotide position 1269 of the reported *P2RY2* cDNA sequence. Substitution of a "C" at this position induces replacement of an arginine residue with a serine at amino-acid position 312 (Fig. 2). To our best knowledge, neither oncogenic activity nor non-synonymous mutations at these sites have been reported.

```
44  C    V    P    G    L
    TGC  GTG  CCT  GGG  CTG
              ↓
    TGC  GTG  CTT  GGG  CTG
44  C    V    L    G    L

310 G    Q    R    L    V
    GGG  CAG  AGG  CTC  GTA
              ↓
    GGG  CAG  AGC  CTC  GTA
310 G    Q    S    L    V
```

Fig. 2. Identification of mutated *P2RY2* cDNA. The nucleotide sequence of our *P2RY2* cDNA was aligned with the previously determined nucleotide sequence of the *P2RY2* cDNA (NM_002564). A single nucleotide change (C to T) at the second position of codon 46 results in a change in the encoded amino acid from proline to leucine. Another nucleotide substitution (G to C) at the third position of codon 312 induces an amino-acid change from arginine to serine.

Confirmation of transforming activity of P2RY2

To confirm the transforming activity of P2RY2(P46L/R312S), we examined its effect on anchorage-independent growth of 3T3 cells in soft agar. Whereas cells infected with an empty virus did not grow in the agar, those infected with a virus expressing P2RY2(P46L/R312S) formed multiple foci in repeated experiments (Fig. 1, middle). In addition, 3T3 cells expressing v-Ras readily grew in the agar.

The transforming activity of P2RY2(P46L/R312S) was also tested by the tumor-formation assay with athymic nude mice. 3T3 cells infected with the empty virus or retrovirus expressing P2RY2(P46L/R312S), wild-type P2RY2 or v-Ras were inoculated subcutaneously into nude mice.

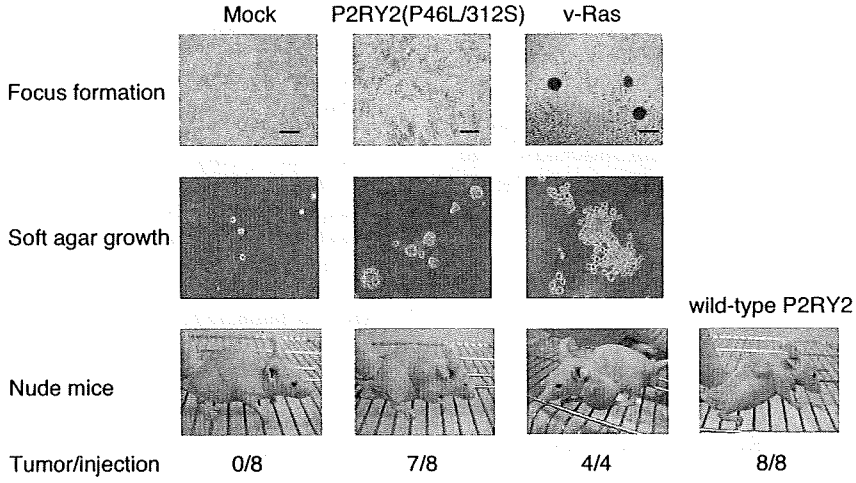

Fig. 1. Transforming activity of P2RY2. Mouse 3T3 cells were infected with empty retrovirus (Mock) or with retrovirus encoding P2RY2(P46L/R312S) or v-Ras, and cultured for 8 days (top). Scale bar, 1 mm. Each cell fraction was also seeded into soft agar and incubated for 10 days (middle). The same cell fractions and 3T3 cells expressing the wild-type P2RY2 were injected into the shoulder of nu/nu mice and tumor formation was examined after 3 weeks (bottom). The frequency of tumor formation determined is indicated.